NAG-2001

Design and Analysis of a 6U CubeSat and Mission

A Major Qualifying Project Report
Submitted to the Faculty of the
WORCESTER POLYTECHNIC INSTITUTE
in Partial Fulfillment of the Requirements for the
Degree of Bachelor of Science
in Aerospace Engineering

by

Tristan Andreani

Samuel Joy

Edward J. Beerbower

Benjamin Snyder

Roberto Clavijo

Jeremiah Valero

Gavin Lee

April 6, 2020

Approved by

Nikolaos A. Gatsonis, Advisor
Professor, Aerospace Engineering Program

Zachary R. Taillefer, Co-Advisor
Assistant Teaching Professor, Aerospace Engineering Program

Abstract

This project presents design and analysis for a 6-unit CubeSat carrying a miniaturized mass spectrometer. The CubeSat is inserted at the International Space Station (ISS) altitude and uses the BET-300-P electrospray thruster to acquire an orbit with perigee at about 200 km and apogee at 440 km.Orbital analysis using the SystemsToolKit (STK) provides an orbital life of about 45 days. STK simulations estimate 17 W of available power and battery capacity of 40 Wh, STK simulations provide the downlink transfer periods with the Near Earth Network and the thermal fluxes onto the CubeSat. COMSOL Multiphysics simulations determine that the induced magnetic fields from the magnetorquers do not adversely affect electronics and sensors.Preliminary design of a thermal vacuum chamber is also presented.

Acknowledgements

We would like to thank the following individuals for their help, support, and contributions to this project.

Project Advisors	Professor Gatsonis Professor Taillefer
Graduate Student Advisors	Harrison Hertlein
Academic & Research Computing Advisors	Adriana Hera
Structural Design Team	Professor Karanjgaokar (Advisor) Brian Kelsey Nicole Petilli Christian Anderson Rory Cuerdon
Attitude Determination and Controls Team	Professor Demetriou (Advisor) Oliver Hassan Chris Renfro David Resmini Andrew Montero Robaire Galliath

Table of Authorship

Introduction	
Background and Literature Review	
CubeSat Applications and Missions	Andreani
Review of CubeSat MQPs at WPI	Joy
Project Goals	All
Design Requirements	
Power	Lee
Propulsion and Orbital Parameters	Snyder, Valero
Telecommunications	Beerbower
Environmental Effects	Clavijo
Overall Project Management	Joy
MQP Objectives, Methods, and Standards	All
MQP Tasks and Timetable	Joy
Payload and Design Implications	Joy
Propulsion Design and Analysis	Snyder, Valero
Power Subsystem Design and Analysis	Lee, Andreani
Telecommunications Design and Analysis	Beerbower
Environmental Effects Analysis	Clavijo, Joy
Thermal Vacuum Chamber Preliminary Research	Andreani
Conclusions and Recommendations	All
Social Impacts	Andreani

Table of Contents

Table of Figures

List of Tables

1. Introduction

CubeSats are small, cost effective satellites which expand commercial access to space. Defined by the standardized Unit (a cube with dimensions of 10cm x 10cm x 10cm, ~1.3kg, denoted 'U'), CubeSats are typically 1U, 2U, 3U, 6U, or 12U. Each Unit is composed of hardware components specifically selected to complete the satellite's mission. The concept began in 2000 as a plan to provide scientific and military laboratories another tool to grow their operations in space. Many colleges and high schools have programs that allow students to design and build their own CubeSats, illustrating that the concept lends itself to valuable educational experience. (Loff, 2015)

This MQP group, alongside its partner MQPs MAD-2001 (Galliath, R., Hasson, O., et al., 2020) and NK-2001 (Anderson, C., Cuerdon, R., et al., 2020), is part of a Systems Engineering Group (SEG) with an overall project goal to perform the conceptual design of a 6U CubeSat. The NIMS eLEO (extreme Low Earth Orbit) Atmospheric Observer (NeAtO) CubeSat is designed to carry a miniaturized Neutral Mass and Ion Spectrometer (NIMS), a proprietary scientific instrument from NASA Goddard for the purpose of scientific experimentation and data collection in the ionosphere (Gatsonis, N.A., Ye, L., et al., 2019).

A solid model of NeAtO is shown in Figure 1. Designed for deployment from the International Space Station (ISS) via NanoRacks at 400km with a 51.6^{o} inclination, the satellite then enters a 200-440km elliptical orbit via a low thrust transfer, maintaining a perigee within eLEO for approximately 150 days. The goal of this MQP is to design and analyze the propulsion, telecommunications, power subsystems, perform payload integration, and perform orbital and environment effects analysis.

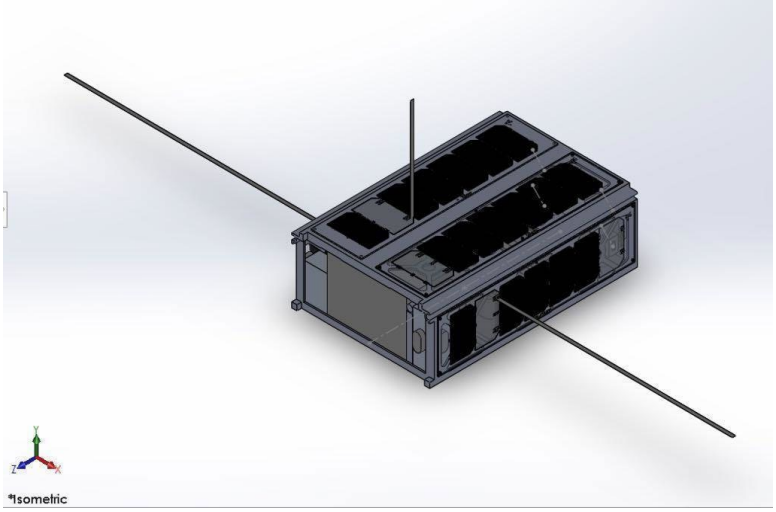

Figure 1 - Isometric View of the NAG-2001 CubeSat, NeAtO

1.1 Background and Literature Review

The following section provides relevant background information and mission objectives. A brief history of CubeSats and their scientific relevance is followed by an overview of previous projects done by Worcester Polytechnic Institute (WPI). The section is concluded by introducing the goals this mission aims to complete for this project.

1.1.1 CubeSat Applications and Missions

In recent years, the CubeSat has become a unique tool in the scientific community. A cooperative culture has formed around the implementation of CubeSats into everyday space science. NASA's CubeSat Launch Initiative (CSLI) provides opportunities to launch small satellites aboard larger launch vehicles as secondary payloads. The industry consists of companies (e.g. Clyde Space, ISIS) providing interested parties with components necessary to construct the satellite, who then work with integration services (NanoRacks, SpaceFlight Services, etc.) to facilitate the satellite's flight aboard a launch vehicle (Loff, 2015).

CubeSats are currently experiencing rapid growth in popularity and technological opportunity. The main advantage to using CubeSats is due to their small size, flexibility of platform design, and simplicity of internal components. Being constrained to discrete sizing of 10cm x 10cm x 10cm units turns the CubeSat into a uniform template for which companies can design consumer off-the-shelf (COTS) parts. This means, if a small scientific payload can be built to fit into a CubeSat, the subsequent mission planning and subsystem creation can be tailored to the payload's requirements. Since 2013, NASA has arranged for 14 CubeSat missions, which utilize their flexibility and design freedom; examples include the Radiometer Atmospheric CubeSat Experiment (RACE) and Interplanetary Nan-Spacecraft Pathfinder In Relevant Environment (INSPIRE). RACE monitors the Earth's water vapor and INSPIRE is a dual-CubeSat communication chain from Mars to Earth that demonstrates CubeSat operation, communication, and navigation in deep space. Once CubeSat operation in deep space has been successfully demonstrated with INSPIRE, their utility can then extend to third viewpoint observations, advanced reconnoitering of exploration sites, and remote monitoring of other missions (JPL: NASA, n.d).

The global CubeSat market was estimated to have a value of $152 million in 2018, which is projected to rise to nearly $375 million. The coming years expect reduced mission costs, a greater demand for data from Earth observation in LEO, and increased opportunity in government, military, and commercial applications (Markets and Markets, n.d). While the future of CubeSats appears to hold countless possibilities, one of their greatest applications is expanding the academic realm with hands-on mission planning and spacecraft design.

1.1.2 Review of CubeSats at WPI

There are several prior MQPs at WPI which focused on CubeSat development. The 2017 MQP CubeSat project "Design and Analysis of the Sphinx-NG CubeSat" (NAG-1701, 2017; MAD-1701; 2017; JB3-1701, 2017) designed a 3U CubeSat with a mission of observing space weather. The SphinX-NG instrument, developed by the Space Research Center in Warsaw, Poland, performed the observations of space weather. This payload monitored the x-rays of long-term solar flux variability, investigated solar features such as inactive coronas, active regions, solar flares, and plasma irregularities, and observed terrestrial gamma-ray flashes, auroral x-ray spectra, and orbital particle fluctuations. This project in turn expanded upon the work of the 2012 and 2013 MQPs which utilized the same instrument. Their CubeSat was designed to be deployed into a circular polar orbit of 600km, and achieved a lifespan of 17.8 years, which would allow the SphinX-NG instrument to perform its scientific duties and provide more than sufficient data collection through such a long lifetime (NAG-1701, 2017).

The 2018 MQP CubeSat project (NAG-1801, 2018; MAD-1801, 2018; JB3-1801, 2018) created two designs for two different objectives. The first part of their mission was to evaluate the feasibility and duration of flights in eLEO (approximately 210km altitude). This team determined a 3U configuration could not successfully produce enough power, instead opting for a custom 4U frame to accommodate enough solar panels (NAG-1801, 2018). Additionally, despite not reaching its desired 90-day orbit, the team succeeded in obtaining a 24-day lifespan and analyzing the effects of eLEO over that duration (NAG-1801, 2018). The second part of the 2018 mission was to test the possibility of maintaining a 100km arc distance between two CubeSats. Achieving this goal would support the ability to use several small satellites rather than a single large one, which would make it easier to replace malfunctioning components and reduce the operation cost. There was no

real conclusion as to whether or not this rendezvous operation could be successfully completed (NAG-1801, 2018).

In addition to MQPs, research at WPI has been extensive (Moorthy et al, 2019; Moorthy et al, 2018; Kewen et al, 2017; Blandino et al, 2016; Gatsonis et al, 2016). The work of Moorthy et al. (2018; 2019) presented the use of the Busek Electrospray Thruster on orbital analysis to extend the lifetime of a Cubesat in extreme LEO orbit. The following list provides the additional sources for CubeSat research originated from WPI.

1.2 Project Goals

This scientific mission uses a mass spectrometer, within a 6U CubeSat (NeAtO) platform, orbiting with perigee in eLEO. Throughout NeAtO's lifetime, the miniaturized NIMS payload will collect data on atmospheric composition in the ionosphere and relay that data to Earth for analysis. The data will be used to analyze atmospheric weather patterns in order to predict the impacts of geomagnetic storms, and to better understand atmospheric irregularities which affect global communications (NASA, 2017). The planned orbit is an elliptical orbit achieved after ISS deployment, with a perigee of about 200 km and an apogee of about 440 km. The major objective of the mission is to maximize the lifespan of NeAtO due to its extended eLEO by modifying orbital parameters and maximizing fuel efficiency of the onboard propulsion system. The desired mission lifespan is 150 days, which will provide the payload the opportunity to capture data across all seasons on Earth.

This project will provide the soft design, supported by analysis, of the NeAtO spacecraft. NeAtO will execute measurements of the atmospheric composition in the ionosphere using the miniaturized NIMS payload. NeAtO will control payload data collection, storage and downlink,

as well as maintain the slightly elliptical orbit required to interrogate the ionosphere. The data will be used to analyze atmospheric weather patterns in order to predict the impacts of geomagnetic storms, and better understand atmospheric irregularities, which affect global communications (NASA, 2017).

The overall mission has several phases; deployment from the ISS (Phase I), detumbling (Phase II), orbit transfer (Phase III) and science (Phase IV). In Phase I, NeAtO will be deployed from the ISS which has a circular orbit at a 410km altitude and an inclination of 51.6°. Once deployed, in Phase II, NeAtO will power on for the first time and automatically eliminate any unwanted spacecraft rotation. Once detumbling is confirmed and communication established, Phase III will begin and NeAtO will shape the orbit to final orbit using onboard propulsion. In Phase IV, the spacecraft will perform measurements of the ionosphere in eLEO until the spacecraft runs out of fuel or the orbit degrades. It will then de-orbit, as required by CubeSat mission guidelines.

The final orbit (Phase IV) is elliptical with perigee and apogee of approximately 200 km and 440 km, respectively, which will allow several layers of the ionosphere to be interrogated. The primary mission objective is to optimize the science and data collection phase, in part, by maximizing the residence time of NeAtO in this orbit. In this phase, NeAtO will experience a significant drag force eLEO, which must be compensated for by the onboard propulsion system in order to persist in eLEO. Drag compensation will extend the mission lifetime; however, the orbit will still degrade due to the high levels of atmospheric drag at this altitude.

1.3 Design Requirements, Constraints, and Other Considerations

As described above, the design of NeAtO includes three distinct MQPs, each comprised of several subsystems typical of spacecraft projects. The following section describes the responsibilities and goals of each subsystem in this MQP team for the NeAtO spacecraft.

1.3.1 Propulsion and Orbital Parameters

The goal of the propulsion subsystem is to provide a mission profile that will allow NeAtO to achieve its scientific mission with constraints of fuel, space and power allowed for this subsystem. Primary propulsion is used for orbit shaping, changing and maintenance. In terms of primary propulsion, the mission profile includes orbit shaping (Phase III) and maintenance in the science orbit (Phase IV). Optimization of orbit shaping maneuver will determine how much propellant will be available to maintain the science orbit, which is the primary mission objective. The Systems Tool Kit (STK) and custom MATLAB programs for low-thrust trajectory analysis will provide initial propellant usage estimates for these maneuvers.

As selected by the MAD2001 MQP (MAD2001, 2020), the NeAtO spacecraft will be deployed from the ISS. As such, the initial orbit in Phase III is circular at approximately 400km, with inclination of 51.6°. STK will provide the time, propellant and trajectory required to execute the Phase III orbit-shaping maneuver. This analysis will determine how much propellant is available to the spacecraft entering Phase IV, which ultimately determines how much propellant remains to extend the science mission and de-orbit the spacecraft; a critical mission objective. Initially, continuous thrust along the velocity vector will be assumed. This analysis may be refined, at which time thruster commands would be relayed to the ADC subsystem team.

The MATLAB program will be used to perform the trajectory analysis for the Phase IV orbit, which includes regions where the spacecraft will experience significant drag. This analysis will provide parameters required by the OBC, which include thruster throttle level, firing sequences and firing durations. Several parameters can be adjusted including apogee and perigee, thrust levels, wet and dry masses, specific impulse, drag coefficients, and many others which affect the propellant usage and thruster firing sequence. Optimization of this orbit will be critical to extending mission life in this phase of the mission.

In order to design and optimize the orbital profiles and maneuvers, several constraints that limit the analysis and propulsion subsystem must be addressed. The first constraint is the small mass and volume of the satellite. To maximize mission lifetime with such a small propellant budget, it is important to avoid any unnecessary maneuvers, especially particularly propellant-heavy ones such as inclination changes. Performing a significant orbit transfer or inclination change requires a large portion of the available propellant, which is impractical and should be avoided when the mission objective does not require it. The second constraint is the significant drag experienced by the spacecraft at eLEO altitudes. This constraint requires optimizing the desired perigee and apogee with fuel requirements in order to maximize mission lifetime and minimize fuel consumption in the orbit transfer and maintenance. The third constraint is the available power throughout the mission. Many of the spacecraft components will require power at various stages of the mission and orbit. The available power, as determined by the power subsystem, will influence onboard propulsion system firing sequences and could impact propellant usage and optimization.

1.3.2 Power

The power subsystem consists of three main elements: the hardware to generate, store, and distribute electrical power; a power budget to manage and distribute the power; and a generation/capacity timeline to support the power draw of the CubeSat throughout the mission. These tasks are interconnected; making progress in one allows for progress in another. Selecting effective hardware will lead to creating a system that can generate enough power to follow the desired power budget.

An initial power budget provides an estimate of how much power each component will draw at various points in the orbit. This first budget guides an initial hardware selection, from which a power profile is created and analyzed. A functioning subsystem consists of hardware that procures a power profile which satisfies the power budget. Should the selected hardware not create a sufficient profile, adjustments must be made to both the budget and the hardware until the subsystem can fully support the mission.

The power requirements of other subsystems can thus constrain the power subsystem: the summation of many components' minimum power draw throughout the mission sets a minimum required power generation. Hardware selection is also constrained, as what is available on the market may not satisfy the power demands of the satellite. The ideal piece of hardware will not exist, and so the system must be designed in a way to optimize its performance. While some of the NeAtO’s components can be managed to only draw power when absolutely needed, many components must operate at certain power levels at certain times, limiting how much the power budget can be optimized.

1.3.3 Telecommunications

The telecommunication subsystem provides satellites with a way to send and receive data. For spacecraft similarly sized to NeAtO, it is not feasible to store data on the payload and the onboard computer until it can be downlinked, nor is it possible to have a downlink network able to continuously receive the data. Thus, it is important to have a system that can effectively provide long downlink periods for the payload's collected data, and transmit this data as fast as can be supported. The mission will only provide useful data as it can be downlinked. The main constraint for the telecommunications subsystem is its power usage. As telecommunications does not directly affect mission lifespan, it would be one of the first subsystems to have its power budget reduced. Limiting the power rate of the subsystem means that the components would operate at lower rates, slowing the speed of data transmission. The ideal optimized telecommunications system sends and receives all relevant information within its access period with the Ground Station Network.

The physical subsystem consists of two components: an antenna, and a signal processing device. The signal processor may be either a transmitter and receiver working together, or a transceiver, which is the two combined into one component. A consideration for the hardware is the frequency of signals it will generate and receive. Higher frequencies can transmit data faster but require more power and more robust hardware (Beasly, 2014). The physical constraints on the telecommunication subsystem are shared with the rest of the CubeSat systems; it must take up minimal space internally, add as little weight as possible to the spacecraft, and not obstruct instruments that operate externally.

1.3.4 Environmental Effects

Extreme Low Earth Orbits (eLEO) are complicated because of their dense atmosphere, high thermal loading, and strong magnetic interference with spacecraft components. Low altitude orbits induce higher levels of drag that will add to the overall vehicle temperature of NeAtO. Adding a heat shield to protect against drag induced heat will not solve all the issues presented by a space environment. Ionized oxygen and thermal radiation from the sun require that the spacecraft structural material must be treated so the aluminum material does not deform or melt. In addition, the components that make up NeAtO must remain within operating temperatures throughout the mission. Even if all components and materials can withstand the space environment, another physical constraint on NeAtO is thermal shock. Thermal shock refers to a quick fluctuation of temperature. The temperature change adds structural stress on each individual component and material in a CubeSat. Each material has a coefficient of thermal expansion (CTE), thus each component will expand and contract at a different rate. This difference can lead to electronic failure even if the components remain in operating temperature range.

Magnetic interference, from the Earth's magnetic field or other sources, can possibly affect the attitude control system and other components. Magnetometers determine the magnetic field strength of the Earth relative to its own coordinate system, predict inbound field vectors, and compute the attitude control inputs required to align the spacecraft with the desired orientation. The spacecraft is reoriented via magnetorquers, electromagnetic rods which produce a magnetic moment against the Earth's background magnetic field. If the magnetic field created by the magnetorquers exceeds the magnetometer's error tolerance, then proper shielding measures must be taken to mitigate interference. Additionally, the magnetorquers cannot be placed too close to electrically-sensitive components such as the onboard computer and the payload's electronic

components, otherwise any internal data storage may be corrupted by the resultant magnetic force. As a result, the strength of the field generated by a single magnetorquer must be determined via computer simulation (using the COMSOL Multiphysics modeling software) in order to provide the Structures team with any constraints on magnetorquer position. Otherwise, magnetic shielding for sensitive components must be considered.

1.4 Overall Project Management and Budget

The NEAtO project consists of three separate MQP teams, each responsible for different aspects of the project as follows:

- Thermal and Mechanical Subsystems and Analysis overseen by MQP NK-2001 (NK1-2001, 2020).
- Attitude Determination and Control overseen by MQP MAD-2001 (MAD-2001, 2020).
- Payload, Propulsion, Power, and Telecommunication Subsystems, as well as Environmental and Orbital Analyses, overseen by MQP NAG-2001.

Each week, the three MQP groups and their advisors met as one Systems Engineering Group (SEG). At these meetings, one member from each MQP team would present the progress their team made within their subsystems and the open issues which had come up over the past week. The MQP advisors and other teams were encouraged to ask questions and comment to clarify any incorrect or uncertain points. The meetings were also used to request, address, and complete open issues.

1.5 MQP Objectives, Methods, and Standards

1. Perform Payload Integration

a) Evaluate when in the orbit the payload turns on and off for its data-collecting intervals.

b) Determine the necessary power and telemetry budget to complete the primary mission.

c) Plan mission operations for the entire life cycle from deployment to deorbiting in order to ensure all subsystems function toward completing the mission objectives.

d) Properly interface the payload with the spacecraft and connect it to the onboard computer.

2. Perform Orbital Analysis

a) Determine the propellant required to transfer from the initial orbit to the desired elliptical orbit

b) Determine the final orbit for the science phase of the mission

c) Maintain the desired orbit for as long as possible.

d) Obtain orbital parameters to analyze the solar flux on the spacecraft to determine power draw, the drag profile on the spacecraft, and environmental effects in eLEO.

3. Propulsion Design and Analysis

a) Determine the amount of fuel and thrust required to compensate for the drag NeAtO will experience in eLEO using the Busek electrospray thruster BET-300-P.

b) Determine the burn time necessary to optimize NeAtO's orbital lifespan to fulfill the payload’s mission requirements.

c) Determine NeAtO's total ΔV and fuel consumption.

d) Determine NeAtO's final orbital lifespan.

4. Power

a) Create a power budget to assign the power distribution to each hardware component.

b) Select hardware and develop a power profile to satisfy the power budget.

5. Telecommunications

a) Identify a viable Ground Station Network (GSN) within the satellite's coverage range that will maximize data transmission.

b) Select telecommunications hardware that complies with its power allowance and NeAtO's structural requirements.

c) Establish uplink and downlink budgets for the payload and other data-handling instruments.

6. Environmental Effects

a) Identify hazardous space agents and their influence on NeAtO's physical integrity and operational performance.

b) Create a thermal loading model of NeAtO.

c) Create a model of the magnetic interference on internal components due to Earth's magnetic field and due to the use of magnetorquers for attitude control.

d) Provide recommendations to protect NeAtO from the identified hazards.

1.6 MQP Tasks and Timetable

The Gantt Chart presented in Figure 2 outlines the timetable this MQP set to complete specific tasks. It was used as a reference for the team's progress.

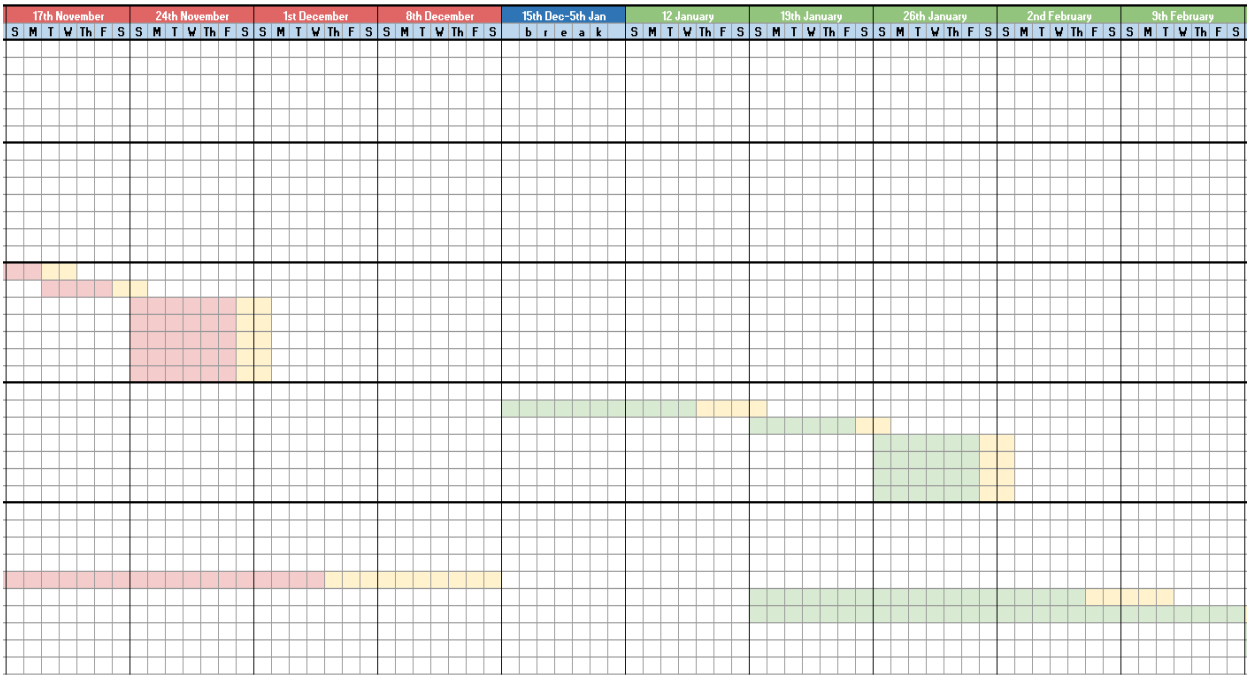

WBS NUMBER	TASK TITLE	TASK OWNER	START DATE	DUE DATE	DURATION	MARGIN	TASK COMPLETE
1	**Familiarization**						
1.1	Learning STK and Certification	Everyone					100%
1.2	ANSYS and COMSOL Training	Everyone					100%
1.3	Read through past papers						100%
1.4	Initial background research						100%
1.5	Sourcing compnents						100%
2	**Initial Estimates and Parameters**						
2.1	Finalize Payload						100%
2.2	Initial Orbital Parameters						100%
2.2	Initial ground coverage estimate						100%
2.2	Initial power budget						100%
2.2	Initial drag profile						100%
2.2	Initial electron flux profile						100%
3	**Revisions**						
3.1	Receive feedback and updates						100%
3.2	Update orbital parameters						100%
3.3	Update ground coverage estimate						100%
3.4	Update power budget						100%
3.5	Update drag profile						100%
3.6	Update electron flux profile						100%
4	**Finalization**						
4.1	Receive feedback and updates						100%
4.2	Finalize orbital parameters						100%
4.3	Finalize ground coverage estimate						100%
4.4	FInalize power buedget						100%
4.5	Finalize drag profile						100%
4.6	Finalize electron flux profile						100%
5	**Paper**						
5.1	Introduction						100%
5.1	Socioeconomic Implications						100%
5.1	Background						100%
5.1	Methodology						100%
5.1	Results						100%
5.1	Conclusions & Recommendations						100%
5.1	Final revisions & edits						100%
5.1	Final formatting						100%
5.1	Submit paper for approval						100%

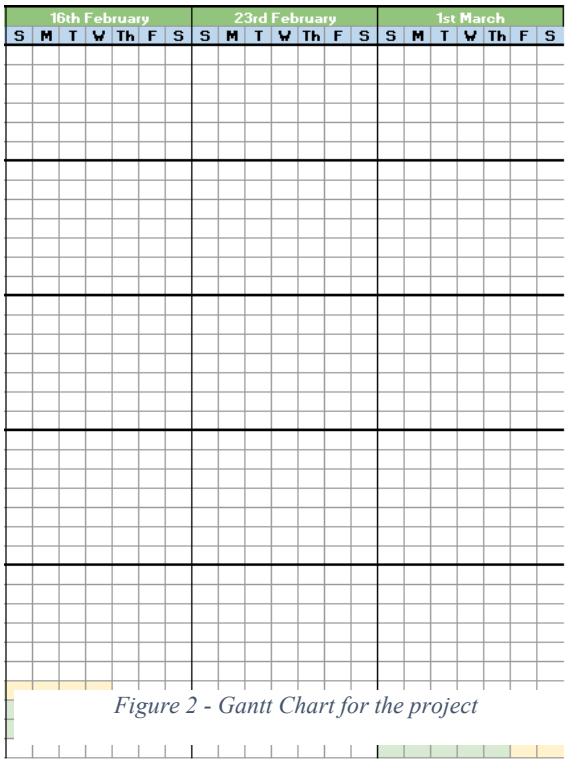

Figure 2 - Gantt Chart for the project

2. Payload and Design Implications

This chapter presents a description of the NIMS scientific payload onboard NeAtO. The payload for a scientific mission is the main driving factor behind mission design and all other subsystems must accommodate its requirements. These requirements, such as orbital position, data transfer and collection, power usage, and pointing characteristics, are outlined below in order to set a baseline for the design of the other subsystems.

2.1 Payload Overview

The payload used on this mission is a miniaturized NIMS provided by NASA Goddard Space Flight Center Heliophysics Science Division (N. P. Paschalidis, 2019). This instrument, shown in Figure 3, requires approximately 1.3U of NeAtO's total volume (13cm x 10cm x 9cm), and provides in-situ measurements of atmospheric composition and density via two apertures aligned with the velocity vector (also referred to as ram-facing), each with a 10° by 10° conical field of view. One of the apertures is specifically dedicated to the collection of ions, while the other has a charged screen to deflect ions and only analyze neutral particles (NASA, 2016). The following section aims to identify notable features of the miniNIMS and how each affects the mission design.

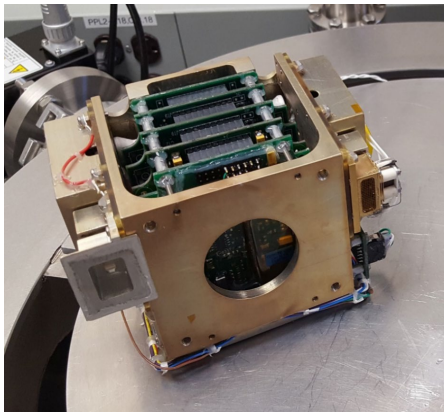

Figure 3 - The miniNIMS used aboard the Dellingr 6U (NASA, 2017)

Aiming to both analyze the dynamic weather of the ionosphere as well as to determine the steady state background atmosphere conditions (NASA, 2016), two CubeSat missions have been launched with the miniNIMS (EXOCUBE-1, Dellingr 6U) and two more launches are scheduled for the near future (EXOCUBE-2, PETITSat). EXOCUBE-1 was a 3U configuration sponsored by the National Science Foundation and developed by the California Polytechnic State University (CalPoly). Launched in January 2015 as a secondary payload aboard ELaNa-X SMAP, it achieved a successful elliptical polar orbit of 470-600km at 98° inclination (NSF, 2013, p. 44). Its antenna failed to deploy properly, resulting in a lower data transmission rate, but in-situ data collection was successful (NASA, 2016). As a result, CalPoly has also developed EXOCUBE-2, which is planned as a follow-up mission to re-attempt EXOCUBE-1, with an estimated launch date of March 15th, 2020 (NSF, 2017).

The Dellingr 6U CubeSat was developed internally by NASA to test its own payload and attempt to build a more resilient CubeSat than most prior models (NASA, 2017). Having launched and deployed in 2017, it has suffered numerous setbacks in orbit, including its attitude determination and control systems and GPS (NASA, 2018), but has been able to recover from these issues and transmit data successfully. The Plasma Enhancements in The Ionosphere-Thermosphere Satellite (PETITSat) will launch in 2021, aiming for a lower orbit in order to explore a regime of 80-400 km, while maintaining the same 6U frame as the Dellingr spacecraft. Specifically, it will investigate the impact of ionospheric depletions (or “bubbles”) and enhancements (or “blobs”) in the mid- and low-latitude ionosphere on global communications (NASA, 2017).

2.2 Consideration of CubeSat Design Criteria

The payload creates many of the parameters and constraints for the mission. The payload requires a ram-facing orientation in order to collect particles through the two apertures, which provides a hard-set attitude to maintain. During data collection, the payload uses 1.8W of power at full operation and collects 13.7kB of data per second, so the data collection period will need to be adjusted to not overburden the power or telecommunications subsystems. To produce meaningful data, the scientific goal driving this mission is to investigate the transition between the F1 and F2 layers of the ionosphere. As such, the orbital perigee must be below the F1/F2 transition altitude (220km), and the apogee must be balanced such that the fuel consumed to achieve the orbit does not significantly shorten the mission lifespan but is not too low to create significant atmospheric drag per orbit.

Before obtaining the payload specifications, the initial suggested orbit and CubeSat size was a 4U configuration - a custom frame from Clyde Space in a 1U x 1U x 4U orientation - orbiting at 250-600km. However, the payload's dimensions are 1.3U x 0.9U x 1.0U, with the apertures on the 1.3U x 1.0U face and would limit the positioning of thrusters. This would force the payload to be aligned with the 1U x 4U face of the CubeSat, massively increasing the expected drag per orbit. The structures team (NK-2001) and this team met to discuss the pros and cons of a 4U versus 6U configuration, and the 6U configuration was determined to meet every requirement for NanoRacks deployment. This configuration will increase surface area by about 43%, allowing for more solar panels, while increasing its internal volume, mitigating internal size constraints and providing more flexibility for orientation of components within the 6U structure. Additionally, this allowed a reduced surface area for drag calculations with the 2U x 1U ram-facing, all at the cost of slightly more mass.

This 6U configuration (2U x 3U x 1U) allowed the payload apertures to point along the ram-facing vector, as it is placed along the lengthwise 2U x 1U face, exactly opposite the thrusters. The original orbit did not cross the F1/F2 threshold either, and the fuel spent for the orbital raise from ISS deployment to a 600km apogee reduced the mission lifespan to 61 days. A new orbit, 200-440km after ISS deployment, was proposed to counteract these two issues, and was analyzed by the orbital analysis and propulsion subsystem teams to improve mission lifespan while allowing the desired data to be captured.

2.3 Determination of Data Collection Period

The NIMS collects data at 13.7kbps uncompressed at the fastest sample rate of 0.1 seconds/sample and with 1.8W of power. NeAtO will use this instrument to collect spectroscopic data of the ionosphere as a function of altitude along each orbit, and as such only needs to collect for, at maximum, half of each orbit - apogee to perigee - to produce a full data set. Approximately 10% of the data transmitted is assumed to be a combination of GPS and IMU data to provide altitude and orientation alongside the spacecraft clock (S-clock) timestamps for each data point. As a result, there is a net 10.37Mb which will contain mass spectroscopy data for processing at ground stations on Earth.

The duration of each orbit for which the payload is activated can be derived from Kepler's 2nd Law of orbital motion as:

$$e = \frac{r_a - r_p}{r_a + r_p} \tag{1}$$

$$E = cos^{-1}\left(\frac{1-\frac{r}{a}}{e}\right) \tag{2}$$

$$M = E - esinE \tag{3}$$

$$M = n(t - \tau), \text{ where } n = \frac{2\pi}{T} \quad (4)$$

solved for t, where e is the eccentricity, r_a is the altitude of apogee, r_p is the altitude of perigee, $r$is the payload activation altitude, a is the semi-major axis of the orbit, $E$is the eccentric anomaly, $M$is the mean anomaly, n is the mean angular motion, $T$is the orbital period, t is the time the payload is activated at, and $\tau$is the time of perigee in the orbit (assumed zero in each calculation).

These calculations provided the data collected per orbit, which was then compared to the daily data budget provided by the telecommunications subsystem, to guarantee all data could be successfully transferred to ground stations. The power used per orbit and the time the payload turns on and off was provided to the power subsystem to determine if all power considerations were met.

The telecommunications subsystem generated a data budget of 11.52Mb per orbit. At 90 minutes per orbit, this results in 184.32Mb of data transfer available per day (approximately 16 orbits). The minimum power condition would be turning the payload on at 240km and off at 200km, as this would capture the transition between the F1 and F2 layers of the ionosphere during daytime. This minimum power condition is important to set a reference point - at only 8.94% of the orbital period, it minimizes not just power usage but also the data sent per orbit. While it saves power by reducing the telecommunications power draw to two-thirds its maximum operational value, this option also produces the least overall data transfer at 105.8Mb per day, or 6.61Mb per orbit.

The theoretical maximum data collection condition would be turning the payload on at apogee (440km) and off at perigee (200km). This theoretical maximum is not achievable with the given telecommunications data budget, producing over double the budget at 591.8Mb per day or

16.44Mb per orbit. As such, the actual maximum is powering on at 292.99km, which uses the entire 184.32Mb per day, and allows for data collection during 15.57% of each orbital period.

Figure 4 shows the data transfer threshold per orbit is shown in red against the curve representing the data collected per orbit at a given activation altitude in blue. The theoretical maximum at just over 290km appears where the curves intersect. The data usage diminishes with altitude at an almost linear rate of 0.9-1Mb less per 10km.

Although this is a scientific mission, certain parameters must be ceded to allow for the operation of the spacecraft. There are reduced power options at slower sample rates, down to 10 seconds/sample at 1.3W, but the power reduction is insignificant while the data produced is drastically less, so the team aimed to maintain this maximum sample rate. Data collection for the entire mission would be ideal, but is infeasible given the power and data transfer constraints. As such, this mission will utilize the minimum power option, which is only 57% of the data potentially collected during the mission, but in turn does not strain the power budget as it reduces the power consumption by both the payload and telecommunications subsystems by 43%.

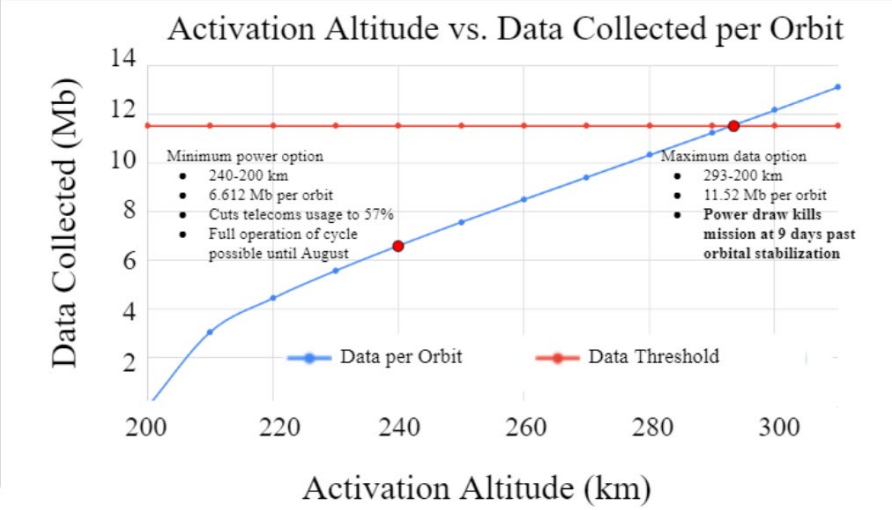

Figure 4 - Activation Altitude vs. Data Collected Per Orbit

3. Propulsion Design and Analysis

This chapter reviews the process of designing NeAtO's primary propulsion system. It consists of an overview of the system hardware and the subsystem's capability of maintaining the desired orbit.

3.1 Propulsion Overview

In previous Cubesat Design MQPs, project scope and analysis were limited to identifying existing possible propulsion options for CubeSats and approximate propellant budgets based on simplified mission profiles and impulsive maneuvers. This general research and analysis provided a comprehensive list of thrusters, which were reasonable to consider for this mission. In some cases, detailed mission profiles were not required, and many of the propellant budget estimates and thruster selections were not based on rigorous trade studies. Some attempts were made to estimate spacecraft mission lifetime in orbits similar to the one considered in this project; however, most did not optimize the entire mission profile to maximize mission duration.

3.2 Busek Electrospray Thruster (BET)

The propulsion system uses the BET-300-P Modular Precision Thruster for primary propulsion. The choice of the Busek thruster was made easy by its size, specific impulse (I_{SP}), thrust, power, and control characteristics. The BET-300-P has been experimentally evaluated as a precision control actuator for small spacecraft (Courtney, Daniel; 2018). These thrusters are relatively small, require no moving parts, contain no high-pressure propellant storage devices, use non-volatile propellant and provide adequate thrust and specific impulse, making them an ideal candidate for the primary propulsion system for CubeSats with low thrust demands. Four thrusters, positioned in the four corners of the 2U x 3U panel opposite the payload, will each provide 5 to

300uN of thrust, totaling a possible thrust range of 10 (two thrusters firing at low thrust) to 1200uN (all four thruster firing at full throttle). Electrospray thrusters such as the BET, or colloid thrusters, are a form of electric propulsion. They use an electrostatic field to accelerate droplets or ions of an ionic liquid (propellant). This type of thruster also has a high specific impulse; however, its thrust capability is orders of magnitude lower than other electric thrusters, such as ion engines - usually only micronewtons (μN) of thrust. This makes these thrusters primarily used for fine attitude control or as primary propulsion for much smaller scaled spacecraft, such as CubeSats ("Electrospray Thrusters Boost Efficiency, Precision." *NASA)*.

Table 1 – Busek Electrospray Thruster Specifications

Thruster head size	5 x 5 x 5 cm
Mass (wet)	230g (not optimized)
Propellant Load	16g
Total Impulse	135Ns
Nominal Thrust	5 - 150uN
Maximum Thrust	300uN
Control modes	Throttleable from <5uN to >150uN
Specific Impulse	2300s
Thrust Control Resolution	<500uN
Thruster head power	2.5W / 6W

3.3 Phase III Analysis and Results

Two legs of the mission profile, Phase III and Phase IV, define the total propellant budget. In Phase III, a ΔV is required to shape the spacecraft orbit from the deployment orbit (ISS orbit) to

the Phase IV orbit (440km X 200 km). In this phase, the orbit is shaped by a continuous low-thrust maneuver using all four thrusters at 250uN throttle level. This maneuver could require a significant fraction of the propellant, leaving little for orbit maintenance in Phase IV, which is the primary mission objective. Thus, proper optimization of this leg of the mission profile significantly impacts the duration of the mission's science phase. Several factors were considered including thruster throttle level, total maneuver time and final orbit shape (the shape of the Phase IV orbit).

Phase III of the maneuver analysis was performed using STK. Preliminary estimates of the initial (ISS orbit) and final orbits (Phase IV orbit) were used with STK to provide an initial propellant budget estimate for the Phase III maneuver. These preliminary estimates were based on a Phase IV orbit with a perigee and apogee of 220 km and 600km, respectively. The preliminary results suggested the Phase III maneuver would consume the entire propellant budget. This would leave little, or no, propellant for the science phase of the mission, thus, the maneuver needed to be optimized to conserve propellant.

The optimized Phase III propellant budget was determined using STK through multiple iterations by manually updating the final orbit. The resulting orbit transfer sequence, which represented the transfer from the ISS orbit (Phase II end) to the final 200-440km orbit (initial Phase IV orbit), consumed 35.194 g of propellant and required 20 days .

A STK finite maneuver sequence was used to simulate the intermittent low-thrust transfer maneuvers, which allows the user to select low thrust levels and the burn is not considered impulsive in the propagation sequences. This sequence allows for low acceleration transfers below $10 m/s^2$. The Phase III orbit transfer can be seen in Figure 5.

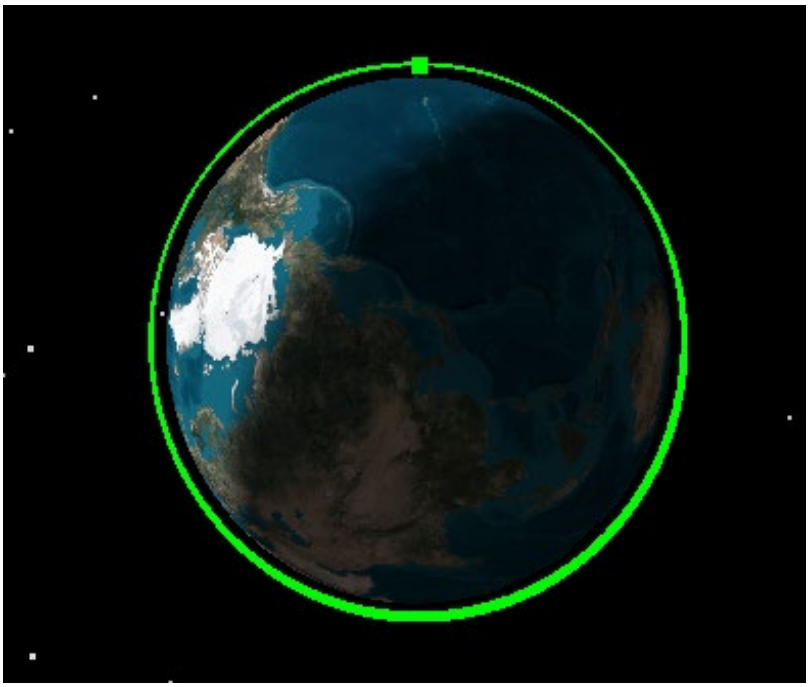

Figure 5 - Overview of the low-thrust orbital transfer

The parameters of the CubeSat used in the simulation are shown in Table 2. The initial orbit is defined using the ISS orbit since NeAtO will be using it as its launch platform. The initial spacecraft parameter values are defined by the structural team, who made a simulation of NeATo where the mass, drag coefficient, and ram-facing surface area is defined. The total tank volume and fuel density is defined by engine specifications.

Table 2 - Parameters used in STK propellant budget simulation

Initial Orbit	Spacecraft Parameters
ISS Orbit	Mass - 6.8kg
Inclination - 51.6°	Drag Coefficient - 4
Apogee - 410km	Area - 0.002m^2
Perigee - 400km	Total Tank Volume - 0.005m^3
	Fuel Density - 1280kg/m^2

These parameters, coupled with the initial orbital insertion parameters, provide an adequate initial state for STK. This initial state condition is used by the STK propagation sections within Astrogator to generate the simulation.

The simulation was completed with two propagation sections, defined by propagation constraints that aim for an apogee and/or perigee parameter constant. These constraints are maintained while the thrust time is varied at apogee and perigee through a component browser. Engine application is defined based on the component browser within STK which are modulated to satisfy the BET engine parameters. However, within the propagation segment, the engine must be defined to have a constant thrust level and Isp throughout the orbital transfer.

During the propagation, the engines were manually defined as either active or inactive throughout the orbit, done by adding constraints to the STK simulation. By varying the active and inactive periods to adjust total fuel consumption, a burn time profile was found that produced a transfer orbit convergent to the desired perigee and apogee that met defined constraints (Phase IV orbit). A detailed description of how to achieve this orbit via auto sequences was found in the "Introduction to Auto Sequences" section of the Level 3 STK help page (AGI Inc.). These propagation segments, through following the steps on AGI's website, were used to calculate the final orbital maneuvers

3.3.1 Orbital Transfer Results

The objective of the orbit transfer analysis is to define thrust vectors and their magnitudes required to travel from the ISS orbit to the 200-440km orbit. These values define the total propellant budget available for orbit maintenance once the transfer is complete. Once in orbit, NeAtO must maintain the perigee for as long as possible with the fuel left over from the orbit

transfer. Minimizing the amount of fuel used during the transfer maximizes the number of orbits the NIMS payload can operate between the F1/F2 ionospheric layers.

The engine being used must be manually defined within STK's component browser. Using the specifications of the BET-300-P found in “Electrospray Thrusters for Small Spacecraft Control: Pulsed and Steady State Operation”, the engine was defined as shown in Figure 6.

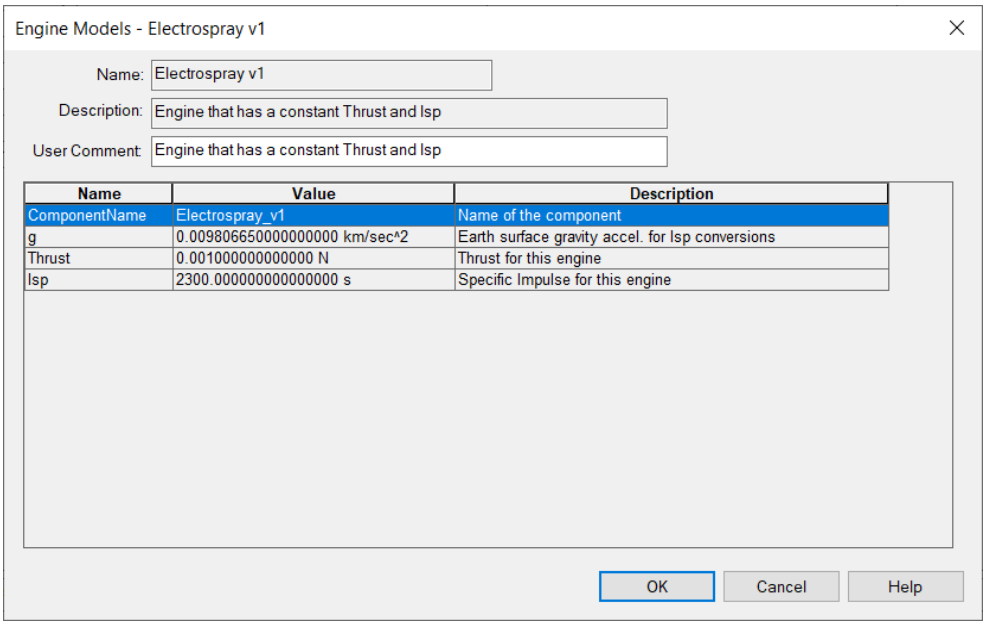

Figure 6 - Engine Model defined in Component Browser

Using the propagation sequence in *Astrogator*, a stopping condition is stated *to* define the automatic engine sequence such as the attitude, engine and propagator of every maneuver performed. The altitude, engine and propagator input values are shown in Figure 7. These parameters define when the engine will be on and for how long. The “Trip Value” seen in the propagator tab in Figure 7 defines how long the engine will be on once it reaches apogee, or perigee.

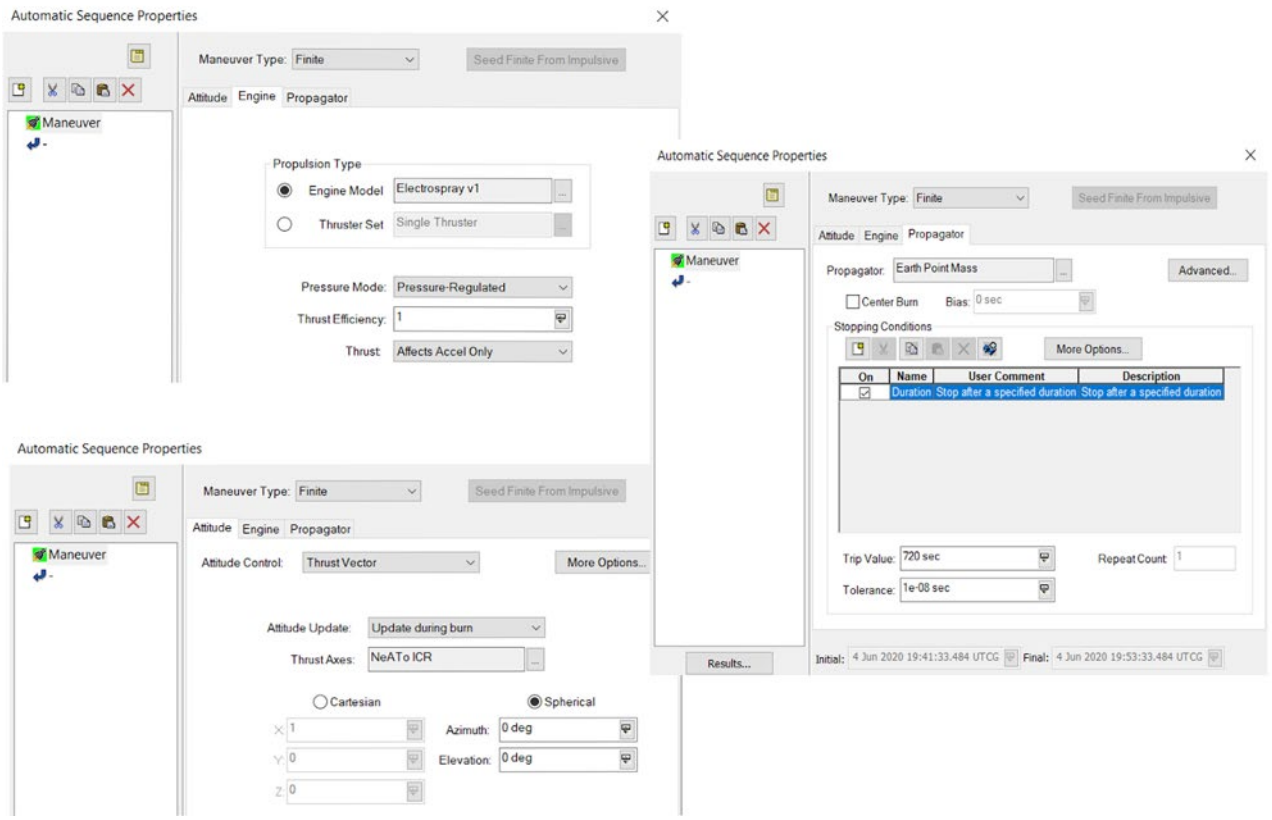

Figure 7 - Thruster Attitude, Engine and Propagator

Once the engine auto sequences are set, the constraints for the propagation are set up. When the program runs the auto sequence to do the transfer, it requires stopping conditions namely the perigee and the apogee of the simulation's final orbit (200km and 440km respectively). An example of the perigee constraint can be seen in Figure 8. The criteria within the constraint is stated in the description of each component.

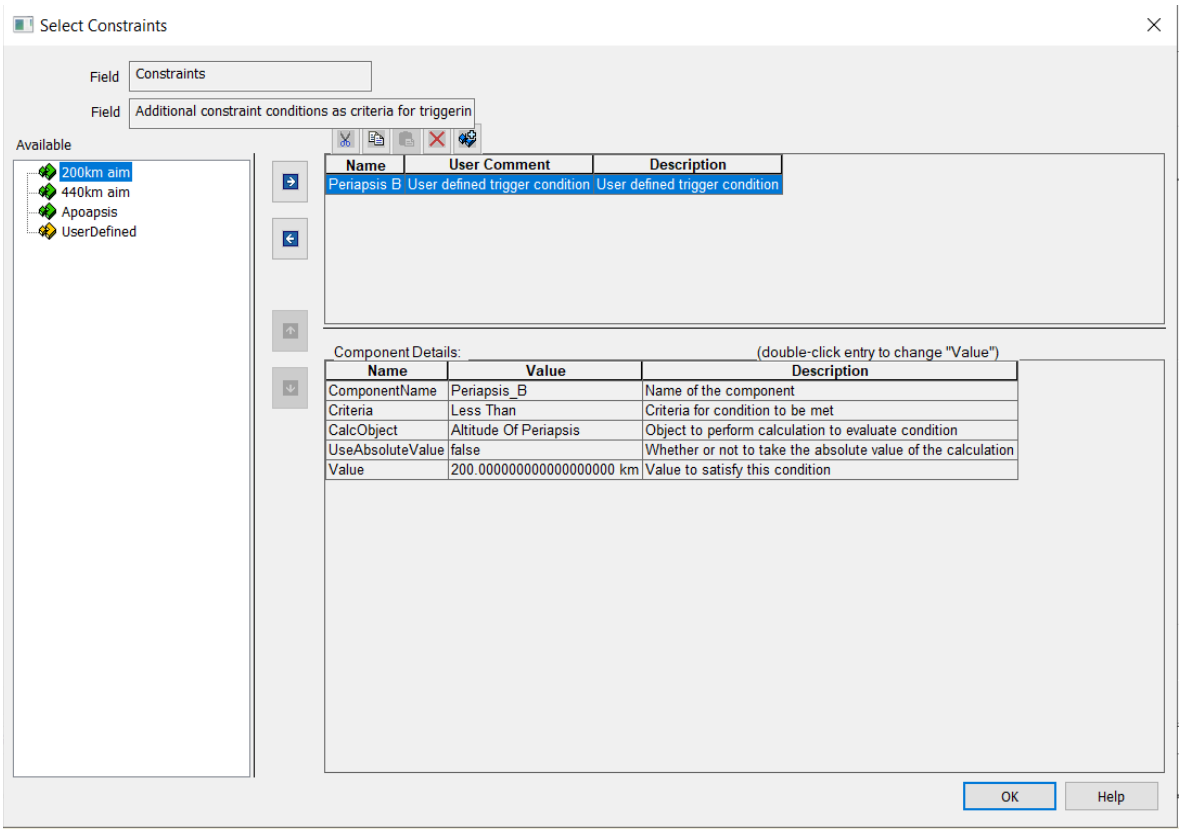

Figure 8 - Thruster Attitude, Engine and Propagator

The Initial State of NeATo seen in Figure 9 is an estimation of orbit insertion after the detumbling phase has been completed and is defined by the initial conditions stated in Section 3.3. The Dual Burn of the program is defined by the stopping conditions in Figure 9 and calculates the necessary thrust maneuvers. These maneuvers are executed until the spacecraft runs out of fuel, encounters an error, or the stopping conditions are met. Iterations of this require varying the Trip Value until perigee and apogee constraints are met.

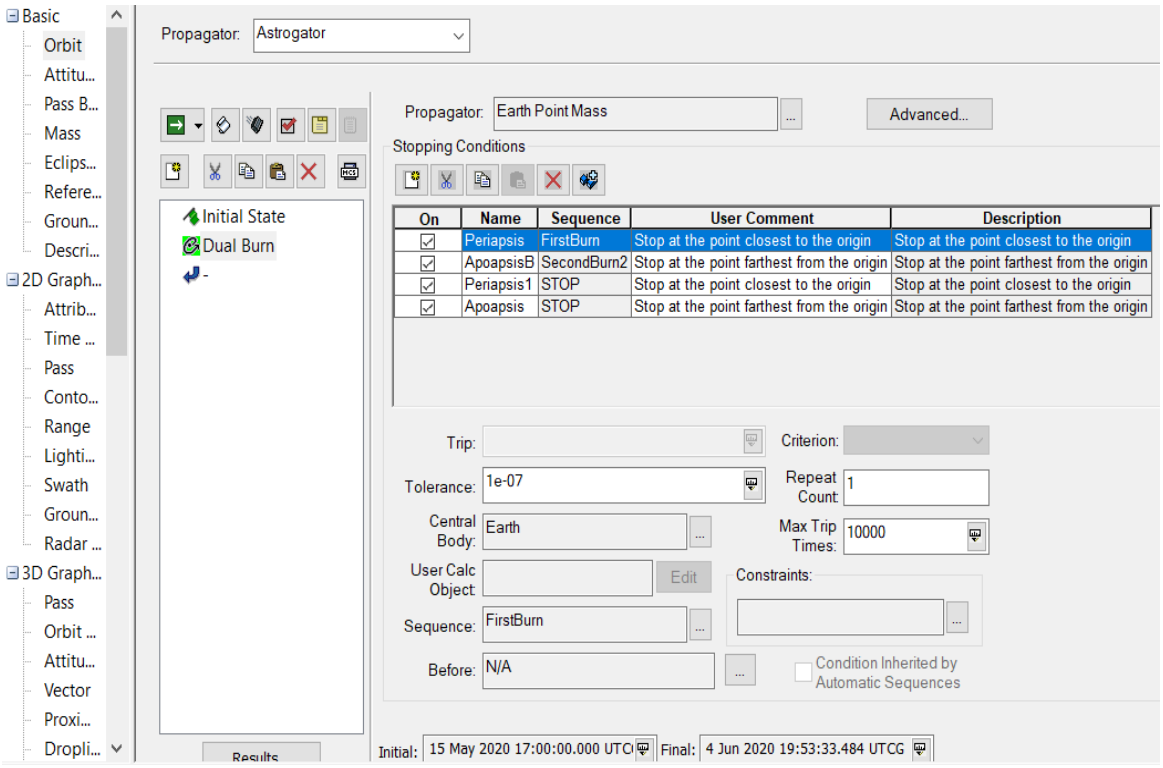

Figure 9 - Stopping Conditions for Orbital Transfer STK

Over various iterations, the Trip Values that satisfied the altitude constraints were 720 seconds at the periapsis and 1800 seconds at the apoapsis. These burn times resulted in a fuel usage of 35.194 grams using the maneuver summary in STK. It is known that NeATo reached the desired insertion point for orbit maintenance by creating a report defining the altitude transfer values by the number of orbits, seen in Figure 10. The figure shows the motion of NeATo, from insertion to the final orbit defined in the simulation. Each line shown in the motion of the spacecraft represents an approximately 90-minute orbit around Earth.

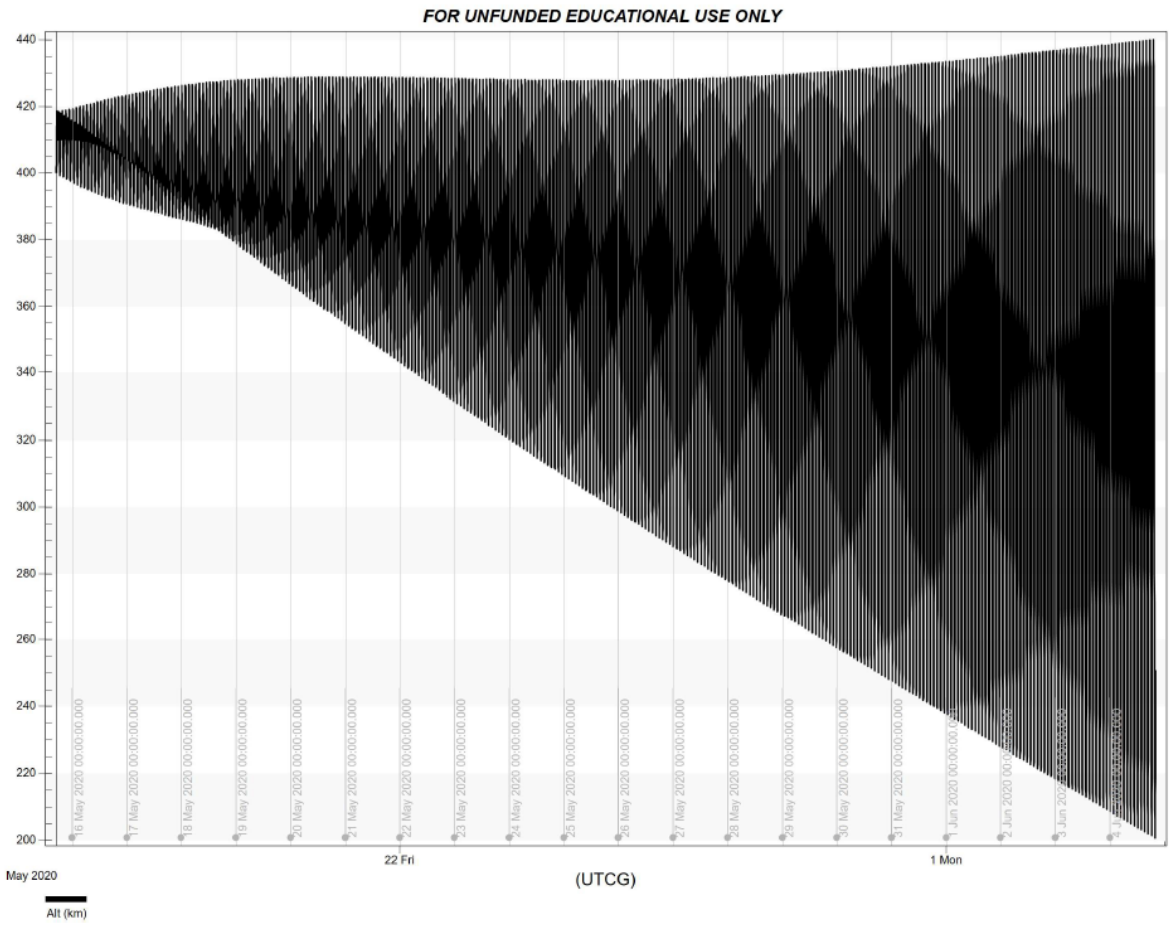

Figure 10 - Graph Showing Orbital Motion of NeATo

This transfer time took approximately 20 days to complete with the engine thrusting for a total of 9.167 days. The total ΔV imparted onto the spacecraft was 115m/s. The final simulation produced a representation of the spacecraft iterations around Earth as shown in Figure 11.

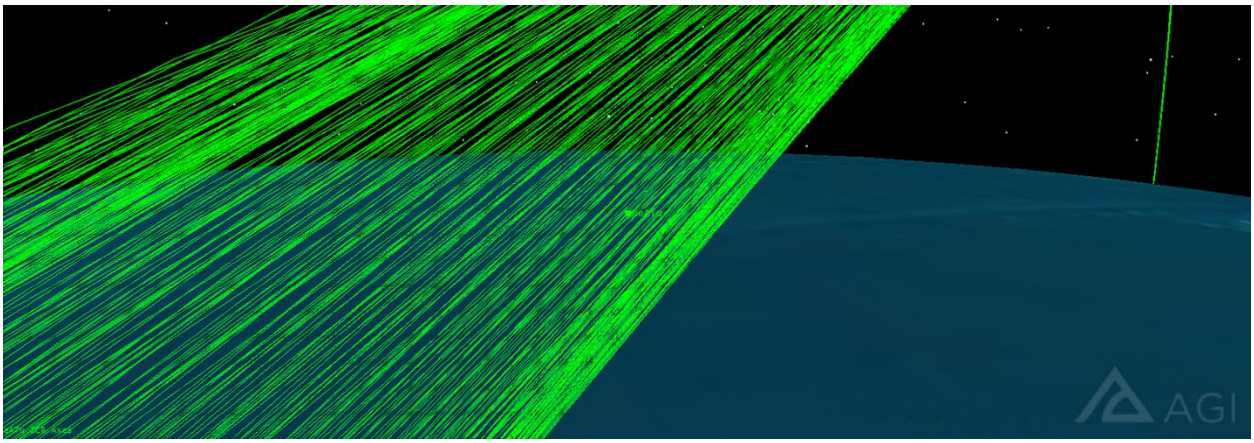

Figure 11 - Image Showing NeATo Iterations Around the Globe

3.4 Phase 4 Analysis and Results

With Phase III computed and analyzed, a proper propellant budget could be obtained. Knowing how much propellant is left after Phase III allows for the NeAtO's final orbit to be optimized. The desired orbit is an ellipse with a perigee at 200km and an apogee at 440km. With such a low altitude at perigee, drag plays a significant role and greatly affects the orbit lifetime. In order to optimize the orbit, an elliptical orbit code was used in MATLAB (Moorthy, 2017). This code allowed the user to change certain parameters about both the orbit, thus simulating the spacecraft flying in a given orbit. Many parameters are required to run the code properly. The altitudes of the elliptical orbit are needed, along with the parameters of the planet the CubeSat is orbiting, which in this case is Earth. Once the orbital parameters are defined, the propulsion system parameters are needed. The specific impulse of the thruster plays the largest role in the code as it defines the efficiency of the thruster. Table 3 shows the simulation parameters to input.

Table 3 – Constant parameters for elliptical orbit code

Apogee	440km
Perigee	200km
Orbital Eccentricity	0.017
Propellant Mass	28g
S/C Dry Mass	6.8kg
Specific Impulse	2300s

In the elliptical orbit code, the parameter *critical radius* defines the altitude at which the primary propulsion system turns on and off. This defines the ignition sequence for each orbit, turning the thrusters on as NeAtO approaches the perigee, and subsequently turn off when it reaches the same altitude after perigee passage. This parameter requires iterations to find the critical radius that will optimize the fuel consumption while properly maintaining the orbit. With an optimized critical radius, the orbit lifetime can be optimized and a full mission profile can be produced.

The critical radius was the first modified parameter. If the critical radius is too close to the perigee, the thrusters cannot generate enough thrust to maintain its orbit; if the critical radius is too close to the apogee, too much thrust will be generated causing the spacecraft's altitude to increase at perigee which means the payload will not be able to obtain its data. Simulations revealed that 250km is the ideal critical radius for this mission.

The controller gain, C, needed to then be adjusted. This value is tuned in order to keep the altitude at perigee as consistent as possible over the course of five periods (Moorthy, 2017). In order to find the optimal value for C, the code was run for a five-period orbit and analyzed for any

significant change in perigee altitude. After multiple iterations, it was decided that a C value of 75 provided the best results. In Figure 12, the altitude is shown over the five orbital periods using C=75.

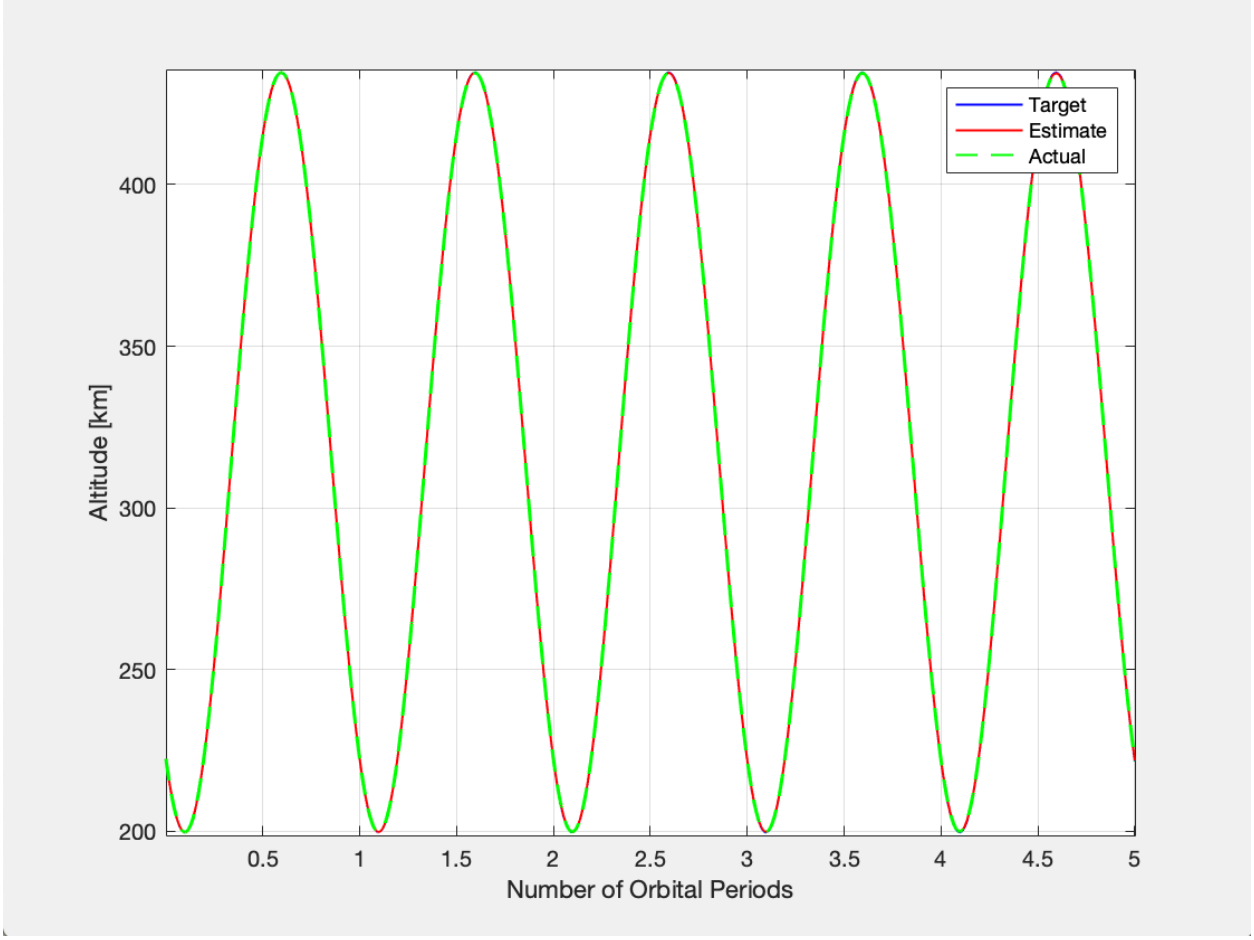

Figure 12 - Altitude over five orbital periods

The minimum and maximum thrust values were first set to the specifications of the BET-300-P thruster. However, these values led to an orbit that would degrade within 20 days. This can be seen in Figure 13, which shows NeAtO's altitude over the number of orbital periods. In Figure 13, the green curve shows the actual altitude over Phase IV; therefore, for a given orbit, the maximum and minimum value of the green curve represents the apogee and perigee, respectively. As the

mission progresses, the perigee (minimum of green curve) decreases gradually while the apogee (maximum of green curve) decreases relatively quickly.

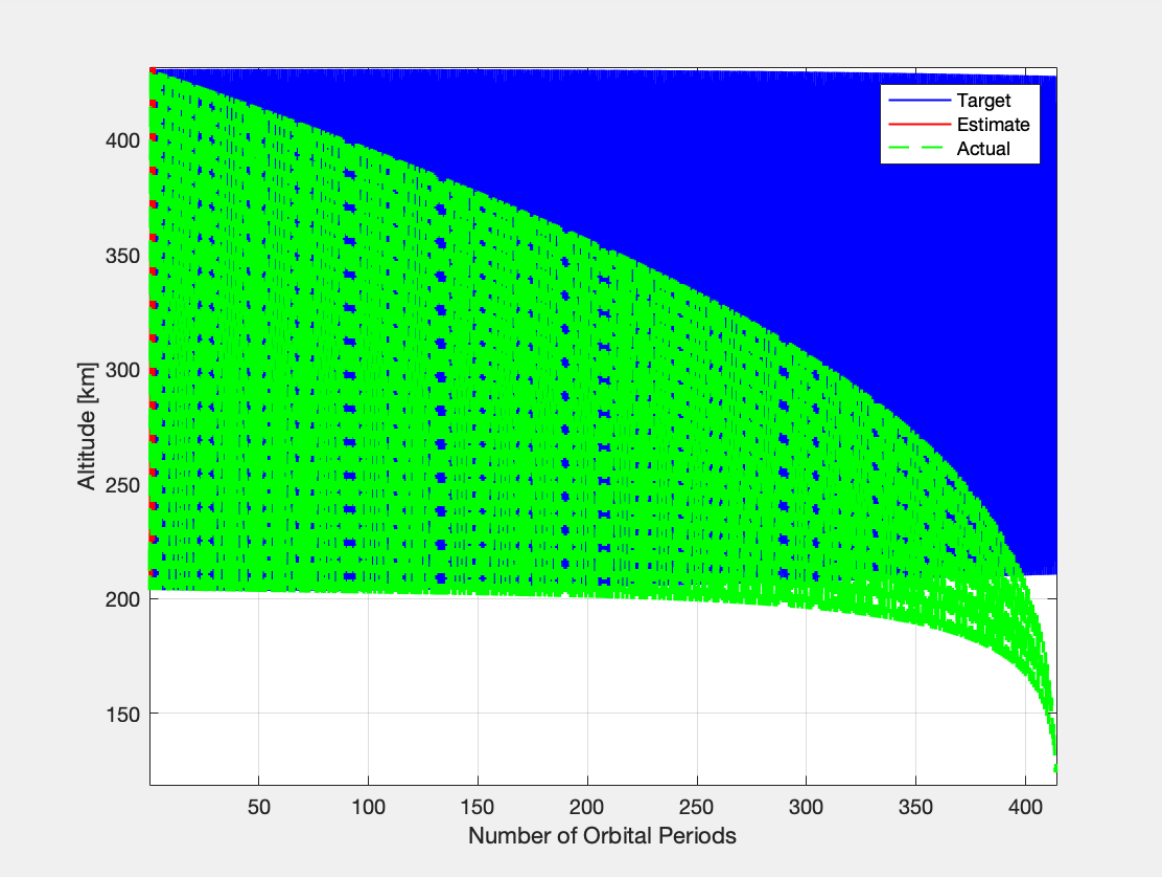

Figure 13 - Altitude vs. Orbital periods; low thrust example

If the minimum thrust exceeded a value above 100μN, the orbit lost its shape and the perigee began to increase in altitude. This orbit may last longer, but the altitude at perigee increases too much for our payload to obtain the correct data needed for the mission. A graph of the altitude against orbital periods for high-minimum thrust can be found in Figure 14.

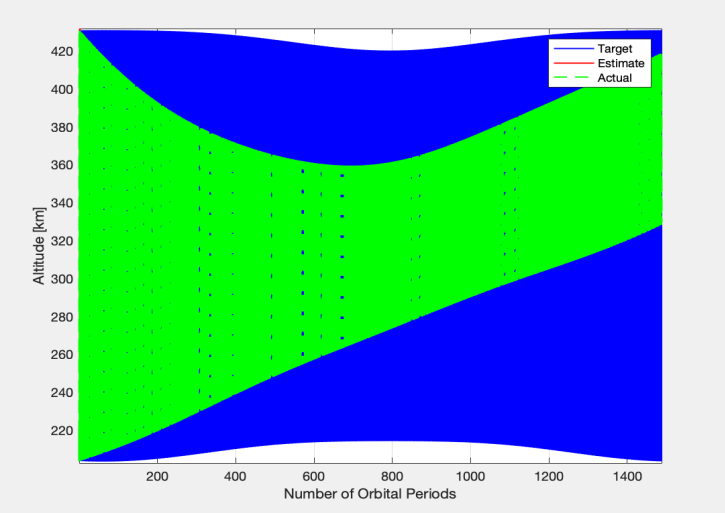

Figure 14 - Altitude vs. Orbital periods; high thrust example

Through numerous iterations with elliptical orbit code to maximize the orbit lifetime without causing the altitude at perigee to increase past 220km, the team was able to find the optimal thrust values. With a maximum thrust of 1000μN and a minimum thrust of 60μN, the orbit lasts for approximately 45 days and keeps the perigee's altitude between 200km and 220km. The altitude graph for this orbit can be found in Figure 15.

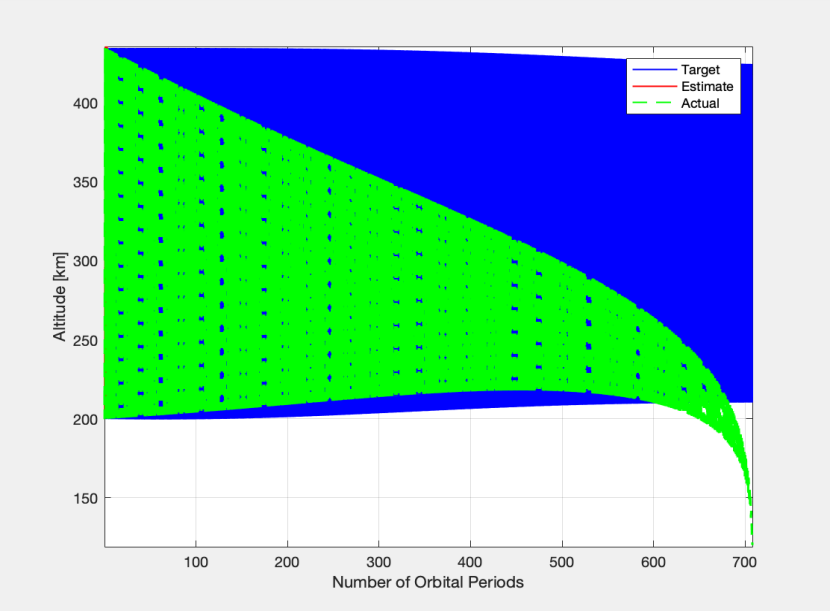

Figure 15 - Altitude vs Orbital Periods for Optimal Orbit

4. **Power Subsystem Design**

The power subsystem is an integral part of the CubeSat. Many of the satellite's components have power needs, and these need to be managed with this subsystem's hardware. As such, a power budget of these component requirements must be created, and a power profile must be generated based on selected hardware in order to accommodate this budget. This chapter lays out the research completed prior to hardware selection, the process by which hardware was selected and the subsystem was designed, and the final results of the power budget and profile alongside what hardware was ultimately chosen.

4.1 Power Subsystem Overview

Since the WPI CubeSat MQPs began in 2010, the selection of hardware components for the power subsystem has been critical in ensuring the operation of the spacecraft for their proposed mission. The previous year's MQP selected hardware for both a 4U and a much larger 16U, each of which performed a separate mission. The 4U from last year's project had a mission into eLEO, similar to this year's. As such, its hardware, all of which is from Clyde Space, provided a baseline for the initial 4U satellite and was even applicable to the 6U redesign. In the event that the team discovered a discontinued component, an updated component was sourced from Clyde Space.

There are two major aspects to designing the power subsystem. First is the CubeSat's power budget, which provides information on the power requirements of other components. Second is the power hardware, which generates, stores, and distributes the satellite's power. A power profile can be created from this hardware, thus allowing one to see if the subsystem can handle the demands of the power budget. The following sections describe how previous WPI MQP projects

designed their power subsystem and which considerations this project took into account for a new design.

4.1.1 CubeSat Power Budget

Power is perhaps the most important resource for a spacecraft, as it allows all electronic components to operate. Due to the small nature of a CubeSat, the amount of power generated by the spacecraft is limited. As a result, accurately estimating power production and consumption becomes exceedingly important to ensure the success of the mission. The previous year's MQP, Design and Analysis of CubeSats in Low Earth Orbit (JB3-1801, 2018), created a table for the 4U CubeSat's power budget with a list of components selected across all subsystems. Their final power budget is shown in Table 4.

Table 4 - Final Power Budget of the 2018 CubeSat for eLEO MQP (JB3-1801, 2018)

Group	Component	Manufacturer	Part no.	Peak Power	Nominal Power	Quiescent Power	Current	Voltage
C & DH	OBC	Clyde Space	01-02928	1	0.35	0.165	150	Batt
ADC	Coarse Sun Sensor	Space Micro	CSS-01	0	0	0	3.5	-
	Fine Sun Sensor	New Space Systems	NSS-CSS	0.05	0.05	0	10	5
	Gyroscope	Analog Devices	ADXRS453	0.04	0.03	0.03	8	5
	GPS	Surrey Satellite Technology	SGR-05U	0.8	0.8	0	160	5
	Magnetometer	Honeywell	HMC5883L	<0.01	<0.01	0	0.1	3.3
Power	EPS	Clyde Space	CS 25-02452	0.2	0.2	0.2	24	Batt
	Battery	Clyde Space	CS 01-02686	-	-	-	2400	7.6
	Solar Panels	Clyde Space	25-02873	-	-	-	-	-
Telecomm	Transceiver	ISIS	TRXUV VHF/UHF	1.9	1.7	0.2	600	6.5-12.5
Propulsion	BET 1mN	Busek		15	10.5	2	-	9-12.6
	PPT	Custom Made		12.5	-	-	-	-

4.1.2 Power Subsystem Hardware

The components that make up the power subsystem need to be able to manage the production, distribution, and storage of power. Due to the small size of a CubeSat, this can become difficult, both because of the limited power generation a CubeSat would have as well as the limited volume to house components within the spacecraft. While various methods of power generation exist for different kinds of spacecraft, the majority of CubeSats use solar panels to generate power and batteries to store the power. In order to distribute power from the batteries efficiently, most CubeSats utilize an Electrical Power System (EPS) board. These boards typically come with Power Conditioning Modules (PCMs), which condition the power into different voltages and currents to be supplied to various components, and Power Distribution Modules (PDMs), which handle which components get power as directed by the On-Board Computer (OBC). As the modules on the EPS continually operate, there is a lower chance for a CubeSat to suffer an electrical failure and thus damage components.

Solar Panels

Power for a CubeSat is typically generated by solar panels due to their simplicity, reliability, and size. Power generation is done by solar cells on each panel, which convert light energy into electricity. The cells are typically made from Gallium-Arsenide, which has a high efficiency and slow degradation, and are then attached to lightweight substrate materials (Wertz & Larson, 1999).

When calculating power generated by a solar panel, one must consider the solar cell surface area, the cell material efficiency, the illumination angle of incidence with respect to the panel, and the operating temperature of the cells. Body-mounted solar panels are fixed to the surface of the CubeSat and gather solar energy proportional to the area they occupy. Deployable panels can be

co-aligned with their mounting surface or deploy outward to optimize the illumination angle and increase total power generation. However, should a CubeSat's orbit dip into the upper atmosphere, deployable panels would significantly increase drag on the spacecraft. Solar cells also degrade and become less efficient over time. Percent degradation is typically low, and thus for a short mission timeline this degradation can be neglected.

The 2018 CubeSat MQP group (NAG-1801, 2018; MAD-1801, 2018; JB3-1801, 2018) required custom manufactured solar arrays from Clyde Space. This was primarily done for design flexibility, as other components also needed to be mounted on the exterior of the spacecraft. Clyde Space no longer provides the manufacture of custom solar arrays; thus, this project aims to identify new hardware to power the mission. At the time, solar panels manufactured by Clyde Space primarily utilized Spectrolab's Ultra Triple Junction (UTJ) Solar Cells which had an advertised beginning of life (BOL) efficiency of 28.3%. Since then, Clyde Space's panels have switched over to using Spectrolab's newer NeXt Triple Junction (XTJ) Prime Solar Cells, which have an advertised BOL efficiency of 30.7%. The dimensions of these newer cells are the same as the UTJ cells, and thus the overall design of the base panels from Clyde Space remains the same should we wish to consider those before considering custom sized panels (Spectrolab, 2018).

Electrical Power System (EPS) Board

The EPS board is a circuit board placed within the CubeSat. As stated above, the function of an EPS board is to control and regulate power via the PCMs and PDMs. The board could be considered a hub; it is directly connected to the OBC, solar panels, battery, and all other components that require power. With these connections, the EPS board monitors power consumption, generation, and storage to ensure the entire electrical system operates at peak performance while also protecting against any hazardous currents and voltages. In addition to this,

the EPS board also keeps the solar panels operating at peak power point, the maximum power generation of the panels based on different voltages and currents. Below in Figure 16 is an example of an EPS board's workflow.

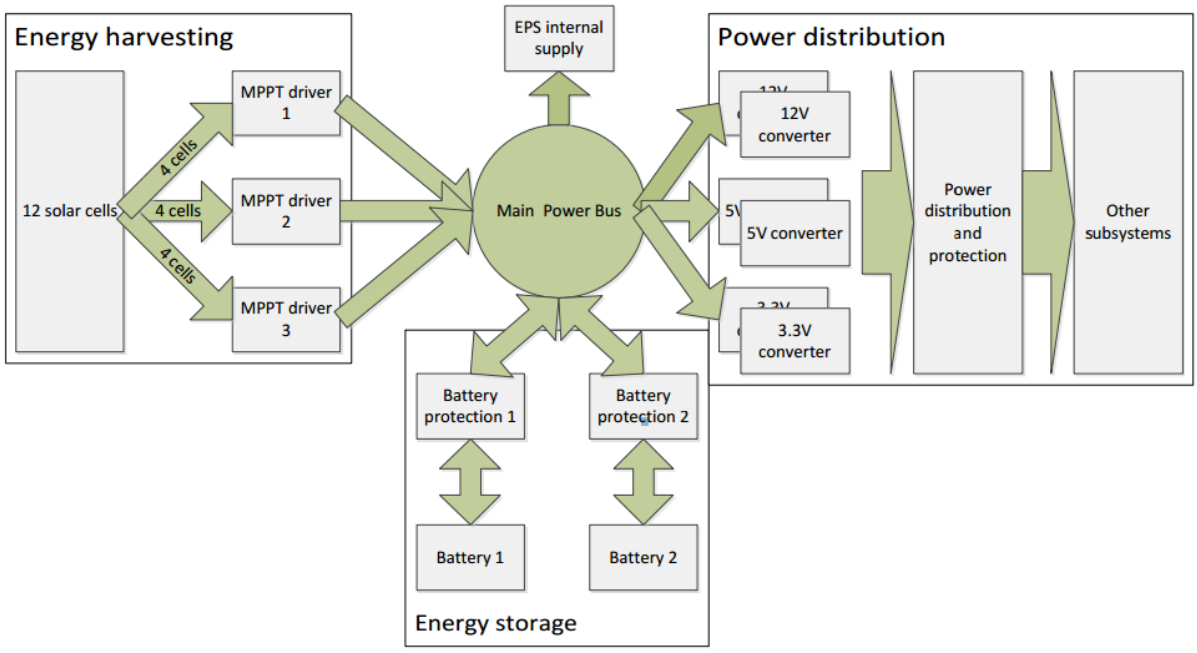

Figure 16 - EPS power distribution (Kalde, 2012)

The 2018 CubeSat MQP group (NAG-1801, 2018; MAD-1801, 2018; JB3-1801, 2018) chose the 3rd Generation 3U EPS from Clyde Space. While selecting this board as a baseline for a 3U or 4U would be ideal (despite the name, the EPS board is compatible with a 4U), there is no mention of this board on the Clyde Space website. It is unclear whether or not this is because it is since outdated or it has simply been renamed, as the naming scheme for the EPS boards available from Clyde Space is now very different.

Battery

Batteries are a CubeSat's primary, and often only, method of power storage. Batteries on spacecraft store power generated by the solar panels while the satellite is in sunlight, and discharge

power while the satellite is in eclipse. The batteries used by CubeSats are secondary batteries, which are rechargeable. This allows the battery to convert chemical energy to electrical energy during discharge and vice versa during solar panel power production.

A primary challenge for designing a CubeSat is managing what limited space there is between required components, such as the battery, with additional components, such as sensors. This can become especially challenging if it's found that a previously selected battery is unable to handle the power requirements of the satellite and thus a larger battery must be chosen. Because interior volume is such a restriction, CubeSat batteries typically use lithium-ion (Li-ion) or lithium-ion-polymer (Li-Po) cells due to their high energy density when compared to other secondary batteries (Wertz & Larson, 1999).

Another major factor to consider is how temperature significantly affects battery efficiency. Compared to other components such as the EPS or solar panels, the battery has a much narrower range of operating temperatures due to the cells used by the battery; both Li-ion and Li-Po cells operate most efficiently between 10^{o}C and 50^{o}C (Navarathinam, Lee, & Chesser, 2011). One way to address this is by using a heater connected to the battery. The battery would discharge while the satellite is in eclipse, and thus would be discharging while the satellite would be experiencing extremely low temperatures. The heater would help the battery discharge more efficiently, as a battery subject to extremely low temperatures will discharge in an exceedingly short amount of time (Horvath, Marosy, Glisics, & Czifra, 2012).

The depth of discharge (DoD), or the percentage of the battery capacity removed, is also an important factor when the battery is discharging. It is important to ensure that the DoD does not exceed the recommended range while the satellite is in shadow. For satellites in Low Earth Orbit,

the average recommended DoD is around 30% due to the number of charge/discharge cycles (Clark & Simon, 2007).

The 2018 CubeSat MQP group (NAG-1801, 2018; MAD-1801, 2018; JB3-1801, 2018) chose the 40 watt-hour battery from Clyde Space. This battery is still available from Clyde Space and is compatible with most of their EPS boards, so it could serve as a good baseline. Clyde Space also has other options if this battery turns out to be unable to sustain this mission.

4.2 Power System Evaluation

Designing the power subsystem entailed first establishing a baseline of the CubeSat's power requirements and constraints. This baseline was determined through researching similar CubeSat missions, namely the two past MQPs. With estimates of the power draw and the surface area constraints of a 4U CubeSat (the mission's initial size configuration before being reassigned to a 6U), further assumptions could be made about the active states of each component. While the mission does not require all components to be active at all times in orbit, making this assumption gave the design team an upper limit estimation of how much power the solar panels must generate. From these initial estimates, the team conducted an iterative process of selecting power components, simulating different flight orientations, and updating the power budget as other subsystems became more thoroughly developed until a satisfactory design was established. Systems Tool Kit (STK) provided all the tools necessary to evaluate the power generation of a particular power subsystem configuration.

4.3 Power Component Selection

The power subsystem is comprised of solar panels for power generation, a battery for storage, and an EPS motherboard for power management and distribution. All components used in past

MQP designs are manufactured by AAC Clyde Space to ensure they are compatible with each other and could be easily integrated onto the CubeSat. The 2018 project used the Clyde Space 3rd Generation 3U EPS board, which included Maximum Power Point Tracking (MPPT), a Power Distribution Model (PDM), and built-in electrical protections. Their battery was the Clyde Space Optimus-40, a 40W-hr battery that could handle higher amperage and come with its own overcharge, over-discharge, overcurrent, overvoltage, and temperature maintenance modules. Lastly, the power was generated by custom body-mounted solar panels with Ultra Triple Junction (UTJ) cells that operated at 28.3% efficiency.

While the team for this current mission used these selections as guidance in the design of the new power subsystem, the EPS board and solar panels have either been discontinued by Clyde Space or only functioned on a 3U CubeSat. Clyde Space no longer offers custom panels, so in their place the team selected Photon-3U panels that operate at 30.7% efficiency (AAC Clyde Space, 2019). Even after the switch over from a 4U to a 6U CubeSat, these panels were still utilized. By setting them on the two 6U surfaces and the two 3U surfaces, these panels can cover approximately 1600cm^2 of the CubeSat's 2200cm^2 surface area. The EPS board was chosen to be Clyde Space's Starbuck Nano-Plus as it includes several internal protective devices and can be easily integrated with the solar panels and battery unit.

4.4 Power Profile Modeling

With all components of the subsystem selected, their performance then needed to be evaluated across the multiple orbital parameters. This required the power generation over all of the considered orbits to be calculated and compared to the power consumption found in the power budget. The power generation calculations were done by creating a model of NeAtO and implementing it into AGI's Systems Tool Kit program (STK). While STK has its own default

CubeSat models that can be loaded into a scenario, their solar panel area and efficiency cannot be edited to reflect the NeAtO's specific hardware. As such, the design team created their own 3D models in the Blender 3D software. Having no prior experience with this software, the team utilized AGI's tutorial resources to create and import the models.

Building accurate models required CAD files of the solar panels, which were received through personal communication with AAC Clyde Space representatives. While having their Zaphod-6U frame would have made for a more accurate model, this file could not be received before the power profile needed to be created, a restriction set by the project timeline. The 3U panels were attached to a simple rectangular prism representing the dimensions of the Zaphod. Each file was loaded into Blender as an .stl file and assigned to their respective places on the CubeSat's main bus. It is important to ensure each panel shared the same coordinate system as the bus.

To designate which areas of the panel will represent solar cells and which will represent the panel frame, each panel must be duplicated and their surfaces deleted so each component reflects their purpose. The surfaces indicating solar cells were deleted on the original panel object, while the surfaces indicating panel structure were deleted on the duplicate objects. Figure 17 shows the Outliner window with complete object hierarchy from the bus to the panels to the cells.

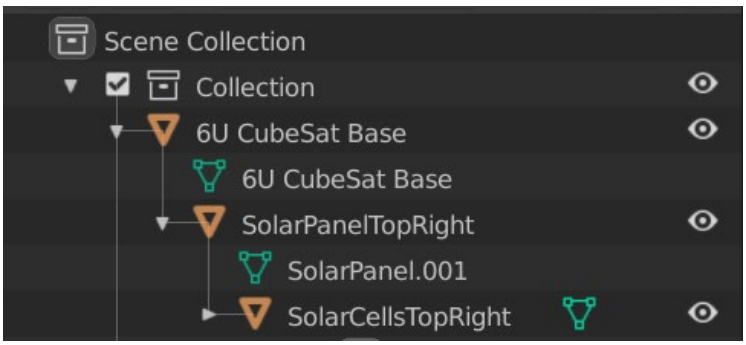

Figure 17 - Example of parented solar panels and cells in Blender

With the model built and saved as a digital asset change file (.dae, necessary for STK integration), there may also be an ancillary file (.anc). To assign solar panel groups and their respective efficiencies, either the .dae file or the .anc files must be edited in NotePad++ according to Figure 18. The ambiguity of which file to edit comes from Blender's propensity to only create .anc files under specific, unknown circumstances. Given both files, they each should be edited accordingly. Figure 19 shows a direct example of edits made to the .dae file. STK's Solar Panel analysis tool will recognize these groups as different solar panels and will create a power generation graph similar to the example shown in Figure 20.

Ancillary Syntax in COLLADA (*.dae)

```
<node id="SolarPanel-PolygonMesh">
   ......................
   <extra type="attach_point">
      <technique profile="AGI">
         <solar_panel group="Ikonos" efficiency="14"/>
      </technique>
   </extra>
   ......................
</node>
```

Ancillary Syntax in Ancillary File (*.anc)

```
<solar_panel_groups>
   <solar_panel_group efficiency = "14" name = "Ikonos">
      <assigned_nodes>
         SolarPanel-PolygonMesh
      </assigned_nodes>
   </solar_panel_group>
</solar_panel_groups>
```

Figure 18 - Edits to be made in Blender-created 3D Cubesat Model .dae and .anc files (AGI Inc.)

```
437        <node id="SolarPanelTopRight" name="SolarPanelTopRight" type="NODE">
438          <matrix sid="transform">1 0 0 0 0 1 0 0.056575 0 0 1 0.0508 0 0 0 1</matrix>
439          <instance_geometry url="#SolarPanel_001-mesh" name="SolarPanelTopRight"/>
440          <node id="SolarCellsTopRight" name="SolarCellsTopRight" type="NODE">
441            <matrix sid="transform">1 0 0 0 0 1 0 0 0 0 1 0 0 0 0 1</matrix>
442            <instance_geometry url="#SolarPanel_006-mesh" name="SolarCellsTopRight"/>
443                <extra type="attach_point">
444                    <technique profile="AGI">
445                        <solar_panel group="Plus_Z_Solar_Cells_Right" efficiency="30.7"/>
446                    </technique>
447                </extra>
448          </node>
449        </node>
450        <node id="SolarPanelTopLeft" name="SolarPanelTopLeft" type="NODE">
451          <matrix sid="transform">1 0 0 0 0 1 0 -0.056575 0 0 1 0.0508 0 0 0 1</matrix>
452          <instance_geometry url="#SolarPanel_008-mesh" name="SolarPanelTopLeft"/>
453          <node id="SolarCellsTopLeft" name="SolarCellsTopLeft" type="NODE">
454            <matrix sid="transform">1 0 0 0 0 1 0 0 0 0 1 0 0 0 0 1</matrix>
455            <instance_geometry url="#SolarPanel_007-mesh" name="SolarCellsTopLeft"/>
456                <extra type="attach_point">
457                    <technique profile="AGI">
458                        <solar_panel group="Plus_Z_Solar_Cells_Left" efficiency="30.7"/>
459                    </technique>
460                </extra>
461          </node>
462        </node>
```

Figure 19 - A direct example of edits made in a Blender-created 3D CubeSat Model .dae file

With the power generation charts, analysis becomes a simple matter of comparing the charts to the power budget. This generation data can be exported from STK into an Excel spreadsheet, and then imported into MATLAB to estimate the battery charge/discharge throughout an orbit. For this team's purpose, the only data imported into MATLAB was the time, altitude, and total power generated by all of the panels. The power generated by each individual panel, while useful, was deemed unnecessary in determining how the battery's overall charge changed over time.

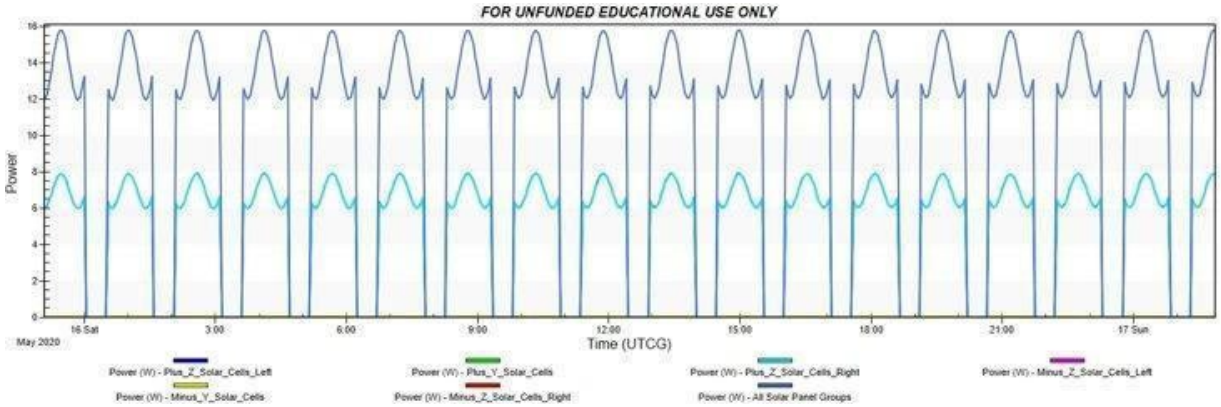

Figure 20 - Sun-synchronous power generation of a 6U ram-facing NeAtO

A script was written in MATLAB in order to compare the data from STK with the power budget. The script first imports and allocates the time, altitude, and power generated data from STK to their own variables before the total power draw and battery charge are determined. The total power drawn over time was determined with multiple loops to simulate the on and off times of each component, as shown in the first section of Appendix A.

The difference between the power generated and power drawn over time was then determined and converted to watt-hours, as shown in the following equations:

$$P_{net} = P_{gen} - P_{draw} \tag{5}$$

$$P_{net,Whr} = P_{net} \cdot \frac{\Delta t}{60} \tag{6}$$

Here, P_{gen} is the solar panels' power generation, P_{draw} is the total power drawn by other subsystems' components, P_{net} is the difference between generating and consumed power, and $P_{net,Whr}$ is P_{net} expressed in watt-hours. All of these values are evaluated at a given time instant. It is important to note that $P_{net,Whr}$ is actually a measure of energy, not power. The variable Δt is the time step, in minutes, that the data was collected in. The charge of the battery over time could then be determined with a loop as shown in the final section of Appendix A. This loop utilized the following equation:

$$E_{battery}(t) = E_{battery}(t - \Delta t) + P_{net,Whr} \tag{7}$$

Here, $E_{battery}(t)$ is the battery's charge at time instant t while $E_{battery}(t-1)$ is the battery's charge at the previous time instant. Effectively what this equation does is it takes the charge of the battery and adds the net power, whether it be positive or negative, in order to determine the new

charge of the battery at the next time instant. A positive net power would indicate that the battery is being charged, while a negative net power would indicate the battery is losing power.

The battery charge could then be plotted as a function of time. Such graphs show two important details: first, the recommended DoD, as stated in the battery section of 4.1.2, must not be exceeded, which can be easily checked upon inspection of the various orbits. Second, if the battery ever reaches 0Whr, then it is clear that the power profile is unable to accommodate the power budget. This can be solved either by improving the CubeSat's pointing in STK, working with other subsystems to revise the power budget, selecting different hardware, or a combination of these options.

4.5 Power Subsystem Results

With the methods of selecting hardware and developing a power profile as outlined above, the team was able to create a subsystem that attempts to meet NeAtO's requirements. Below is an outline of the final hardware configuration and the results of the final power profile.

4.5.1 Final Hardware Configurations

The hardware used for the CubeSat's power subsystem was determined early in the design process. After analyzing the performance capability of each selected component, alternative components were tested to determine if they met the subsystem requirements more effectively. Ultimately, however, no hardware was switched out from our initial selection.

The choice for the solar panels was Clyde Space's Photon-3U body mounted panels (AAC Clyde Space, 2019). When we were initially designing a 4U CubeSat, these were selected because Clyde Space no longer provides custom manufactured panels, as they have in years past. Deployable panels were not considered due to the high drag environment the CubeSat would be

exposed to during its mission. When the switch was made to a 6U CubeSat, the 3U panels were kept, though we did request models of Clyde Space's Photon-6U panels for the 3U x 2U sides. These panels would increase the total solar cell area on the satellite's 6U surfaces, thus generating more power. However, the team had not received such models in time to do a full analysis on them and thus the Photon-3U was simply attached along NeAtO's eight 3U columns.

The final choice for the EPS was the Starbuck Nano-Plus from Clyde Space (AAC Clyde Space, 2019). This part was selected as it would be easy to integrate with the other Clyde Space components. Moreover, it is the only EPS board the company advertises for CubeSats between the sizes of 3U and 12U. The board itself offers complete control over power distribution and conversion. It includes MPPT, a PDM, and protection from overcurrent and under-voltage.

The Optimus-40 40Whr battery, again from Clyde Space, was ultimately chosen to store power. It's operating temperature sits within the range of -10^{o}C and 50^{o}C, which the thermal team took into account in their analysis (AAC Clyde Space, 2019). Once the swap over to a 6U CubeSat had been made and the other subsystems had provided their initial power requirements, the power profiles showed that the charge of the 40Whr battery completely depleted within a matter of days, thus the Optimus-80 80Whr battery was also considered. However, when running the same profile models with the Optimus-80, it was found that the 80Whr battery did little more than to extend the lifetime of NeAtO's's mission by only a few days, indicating that the battery's storage capabilities were not the problem as will be discussed in more detail in the following section. Suffice it to say that once the necessary solution had been found, it was determined that the Optimus-40 battery was able to handle the new power requirements.

4.5.2 Power Profile Results

Determining the orbit that led to optimal power generation consisted of simulating and comparing different power profiles over various orbits. As we had made our hardware selection early on in the design process, we were able to simulate these orbits while waiting for the other subsystems to provide how much power their components drew and when in the orbit they drew it. With that said, none of the power profiles, including the final profile took into account the initial maneuver phase or the orbital decay shown in the results of Section 3.5.2 due to the project's time constraints.

For the final 220-400km orbit, it was found that the panels generated a peak of 17.5W every orbit, as shown in Figure 21. This is not a constant peak power over the entire mission, however, as approximately 80 days into the mission there is a gradual dip in power that eventually leads to a total loss of about 2W in peak power generation, as is illustrated in Figure 22. It was determined that this drop in power generation is due to the sun vector slowly becoming parallel to the body's x-z plane. This means that neither of the panels on the 3U x 1U faces were producing their typical 3.5W of power.

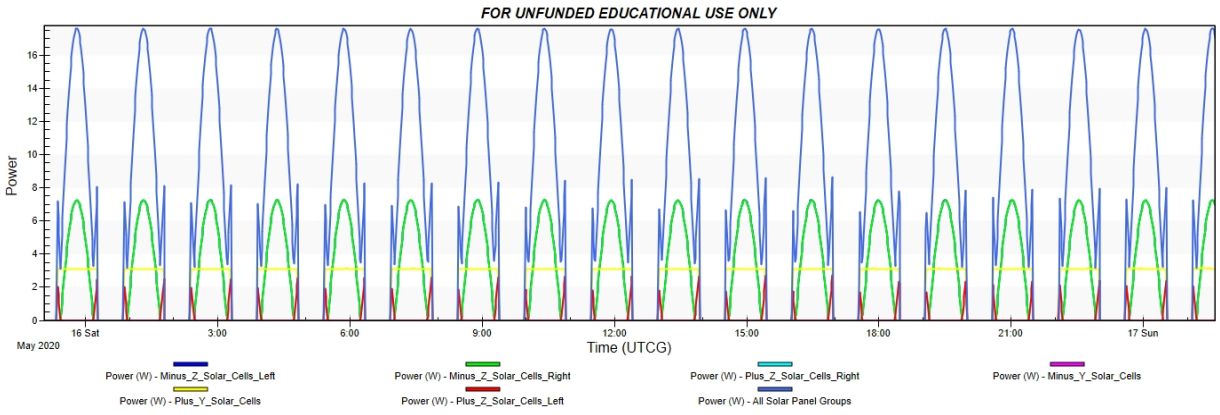

Figure 21 - NeAtO early power generation over a single day

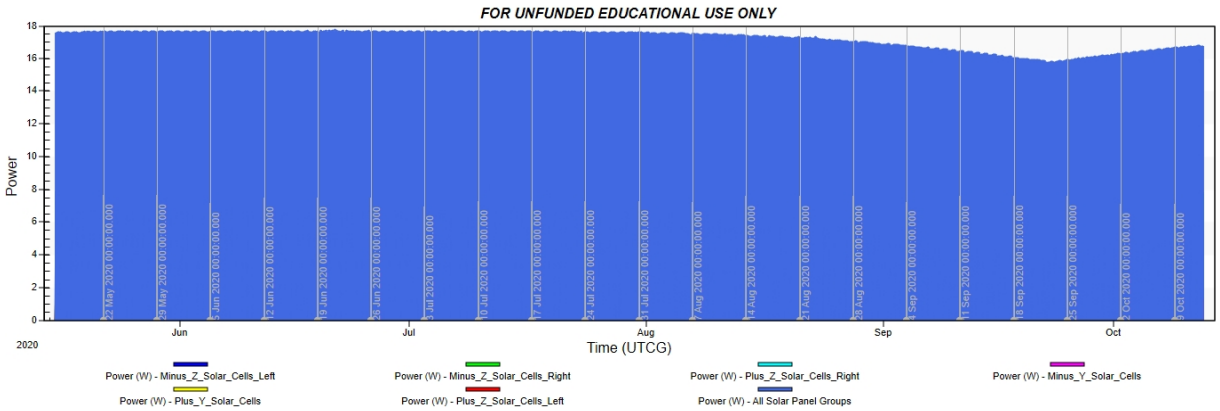

Figure 22 - NeAtO early power generation over 150 days

A battery charge/discharge was initially determined using the power profile in Figure 22 once all the other subsystems had provided their components' power states.. It was found that the selected power hardware would not be able to meet the demands of the other subsystems. The solar panels did not generate enough power and the battery was completely drained after only nine days. Switching the battery to the 80Whr battery from Clyde Space extended NeAtO's lifetime to thirteen days. While deployable solar panels would increase power generation, they were not considered due to the high drag they would induce. The solution was to revise the power budget. In the end, the telecommunication subsystem’s power draw was reduced by 1/3 from the original baseline. The final power budget is displayed in Table 5.

Table 5 - NeAtO's final power budget

Group	Component	How Many?	Peak Power	Nominal Power	Quiescent Power	Peak On-Time	Nominal On-Time
Telecomm	Transceiver	1	4	0.48	N/A	Based on coverage times, ⅔ of orbit	Never
	Antenna	1	2	0.04	N/A	Based on coverage times, ⅔ of orbit	Never
Payload	NIMS	1	N/A	1.8	N/A	N/A	From 240km to 200km
Propulsion	Engine	4	6	2.5	0.5	Never	Never
ADC	GPS	1	1.5	N/A	N/A	Always	N/A
	OBC	1	1	0.4	N/A	Never	Always
	Reaction Wheels	3	1	N/A	N/A	Always	N/A
	Gyroscope	1	0.02	N/A	N/A	Always	N/A
	Fine Sun Sensors	5	0.01	N/A	N/A	Always	N/A
	Accelerometer & Magnetometer	1	0.005	N/A	N/A	Always	N/A
	Magnetorquer	3	0.2	N/A	N/A	Always	N/A

With a complete, trimmed power budget, the optimal power profile was found to maintain a fully charged battery for much of the mission. The Optimus-40 could handle this power draw until early August, when the solar panels began to produce less power. At that point, the battery slowly discharged as provided power to other components; in other words, the solar panels could not generate enough power to charge the battery faster than it discharged. It was initially believed that

this loss in battery charge was due to the lesser power being generated by our solar panels in August. Simulations were rerun within STK using a different pointing orientation for the NeAtO to test this hypothesis. Instead of being ram-facing and nadir aligned, the satellite was instead set to keep its ram-facing orientation while being aligned so that a 62° angle was kept between its body y-axis and the sun vector. This specific angle was selected as it was found to be the angle the satellite kept until the dip in power generation began the 150 day simulation. The results of our final simulation, both over a single day and over 150 days, are shown in Figures 23 and 24 respectively.

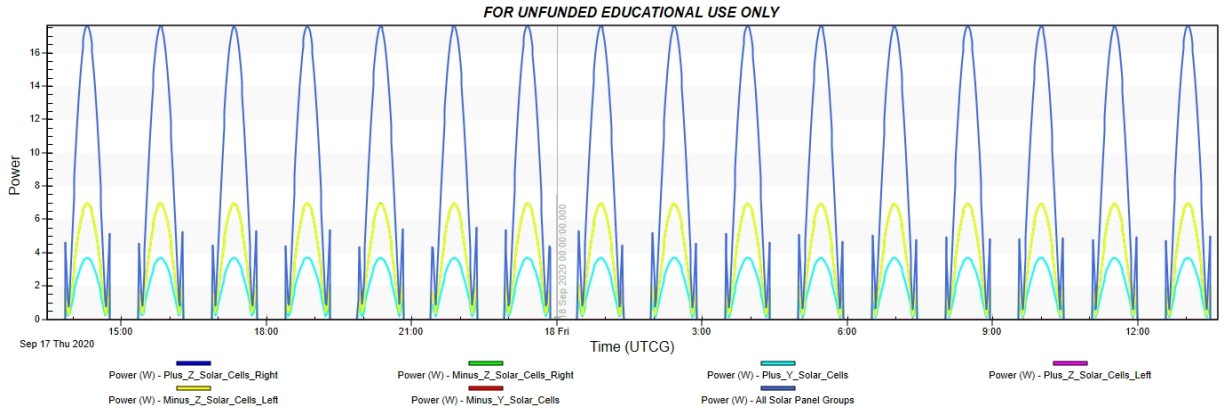

Figure 23 - Final power generation over a single day

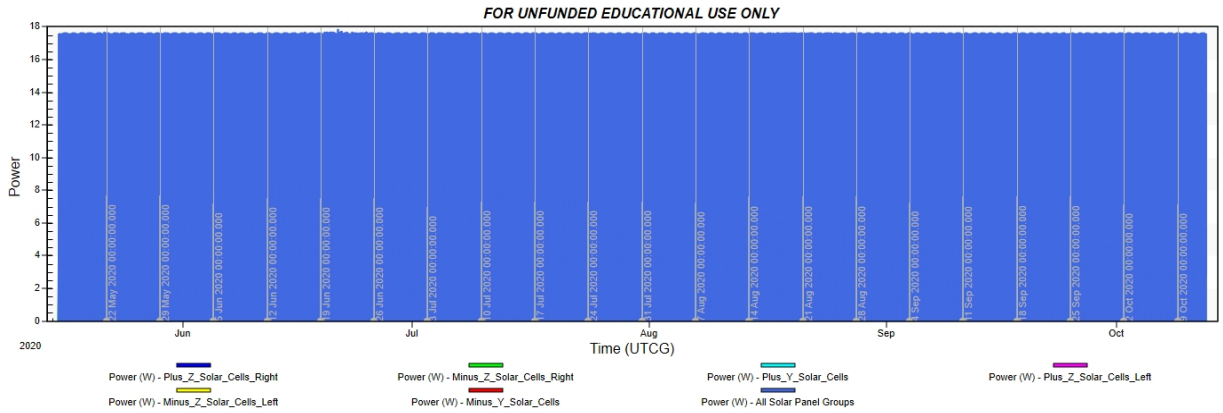

Figure 24 - Final power generation over 150 days

Our final power profile was created using the data in Figure 24. The charge of the battery over a single day early in the mission can be seen in Figure 25. While the battery's charge fluctuates to different maximums and minimums with each orbit, it does recharge to 40Whr every couple of orbits. However, as can be seen from the battery's charge over the full 150 days in Figure 26, improving our power generation later in the satellite's lifetime did not keep the battery from completely draining. While the battery does not reach 0Whr as early as our previous models, it does reach it by August 13th.

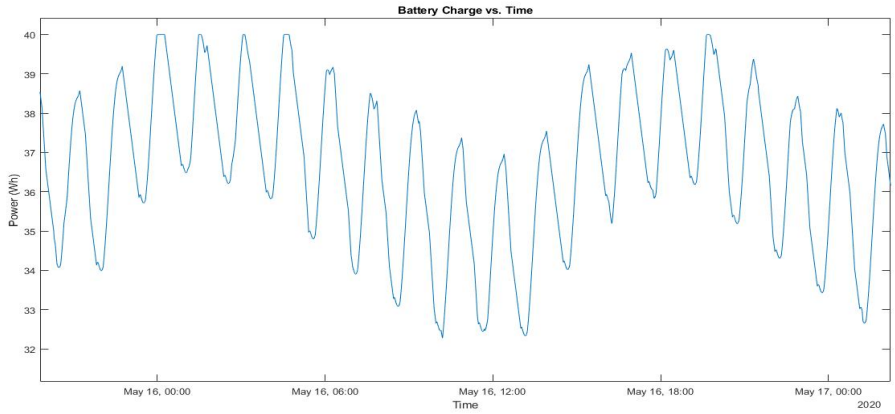

Figure 25 - Battery charge over a single day

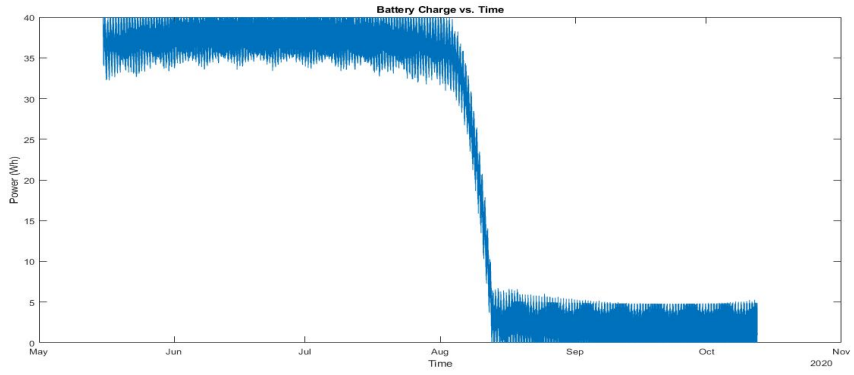

Figure 26 - Battery charge over 150 days

While total power generation did lead to the sudden drop off in the battery's charge, another logical reason lied in the change in altitude that power is generated over the course of the spacecraft's lifetime. Earlier in the spacecraft's lifetime, peak power generation occurs as NeAtO approaches perigee in every orbit, as can be seen by the offset of the power wave with the altitude measurements in Figure 27. However, as time goes on, the solar panels start generating peak power closer and closer to when the satellite is at apogee. This is best illustrated when looking at the power generated and the altitude in mid-September, as shown in Figure 28, where the system had reached its lowest peak power production in previous simulations.

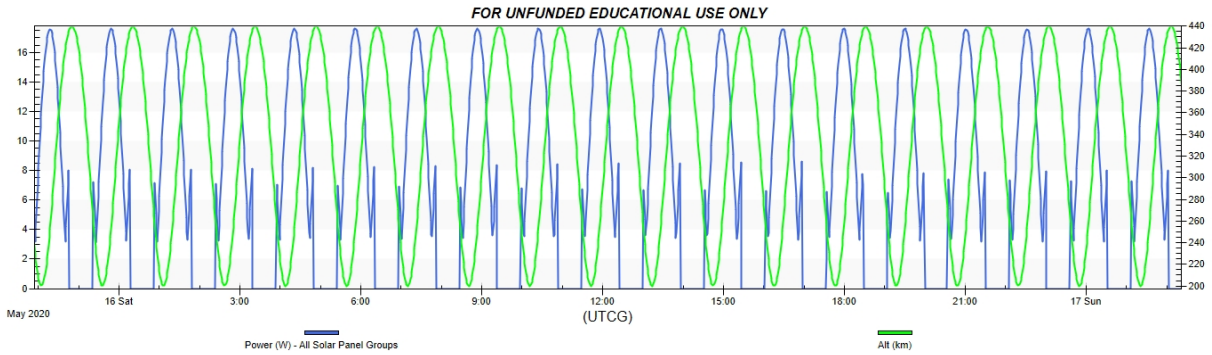

Figure 27 - NeAtO's altitude and power generation over a single day early in the mission

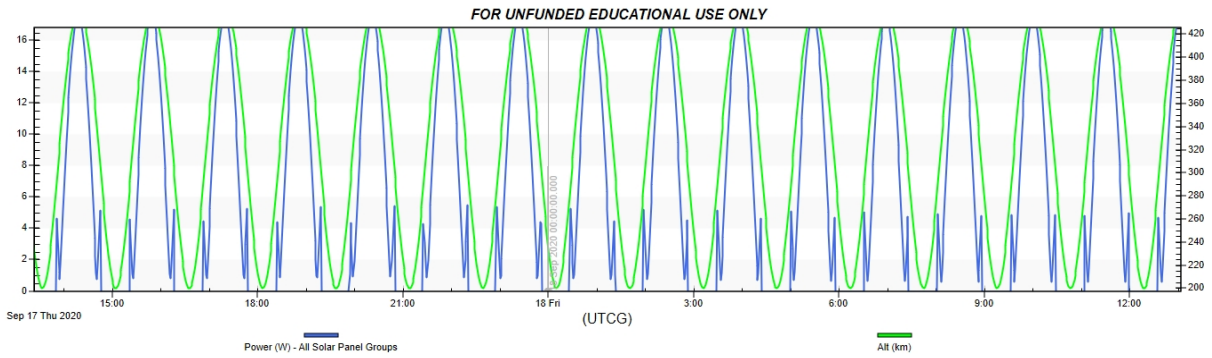

Figure 28 - NeAtO's altitude and power generation over a single day later in its lifetime

Since the times that components require power do not change, this means that as the mission goes into the later months, more and more power is being taken from the battery and not directly from what the solar panels are generating. Eventually it reaches the point shown in Figure 28 where

the peak power generation occurs at apogee, so the bulk power draw is occurring when there is no power generation and is thus directly draining the battery. This unfortunately leads to a situation where the solar panels simply are not capable of recharging the battery as much as it is discharged.

Had the initial detumble and maneuver phases and the orbital decay (Section 3.5.2) been taken into account, all of the results, from the total generated power to the battery's lifetime charge, would have invariably been worse for the mission, though more accurate. Generated power would vary significantly during detumbling, yet certain components would likely have different power modes and/or operating times. During the maneuver phase, the generated power would likely be similar to the current results; however, the thrusters would draw significantly more power and have different active times as they perform their transfers. As for the orbital decay NeAtO experiences, it is likely the drop off in power would occur sooner as the components that turn on when approaching perigee would be in use more frequently.

5. Telecommunications Analysis

The telecommunications subsystem provides a means for NeAtO to receive signals and send data and is comprised of two parts; the hardware on the CubeSat, and the ground stations which receive data. This chapter describes the entire subsystem in detail, how it was selected, and the estimated performance.

5.1 Telecommunications Overview

NeAtO's baseline telecommunications system is designed based upon the equipment used in previous CubeSat projects at WPI. The previous eLEO project, JB-1801 *Design and Analysis of CubeSats in Low Earth Orbit*, chose a VHF/UHF Duplex Transceiver and Dipole antenna from Innovative Solutions In Space (ISISpace). Both instruments operated within the S-Band radio frequency spectrum.

As for the ground stations, past teams considered a variety of stations, professional and amateur, including the option of creating a mobile ground station to customize and expand access points. They also compared various orbital inclinations to find which provided the most access coverage. It was concluded that an orbit with the same inclination as the ISS (51.6°) was the best (JB-1801).

Research in the current project focused on finding newer technology and alternative hardware options, which could improve the subsystem performance and allow for different setups of the CubeSat.

5.1.1 Coverage

The coverage network is extremely important to the success of the telecommunications subsystem, as such, a reliable and professional network is a high-priority figure of merit when determining ground stations to communicate with any satellite. The NASA Near-Earth Network (NASA NEN) is therefore an excellent candidate, due to its extensive history and strategic station placement, and was used in the previous WPI CubeSat project. Figure 29 shows the stations comprising the network, and coverage for a 51.6º inclination orbit. The NEN is detailed in the Nasa Near Earth Network User's Guide.

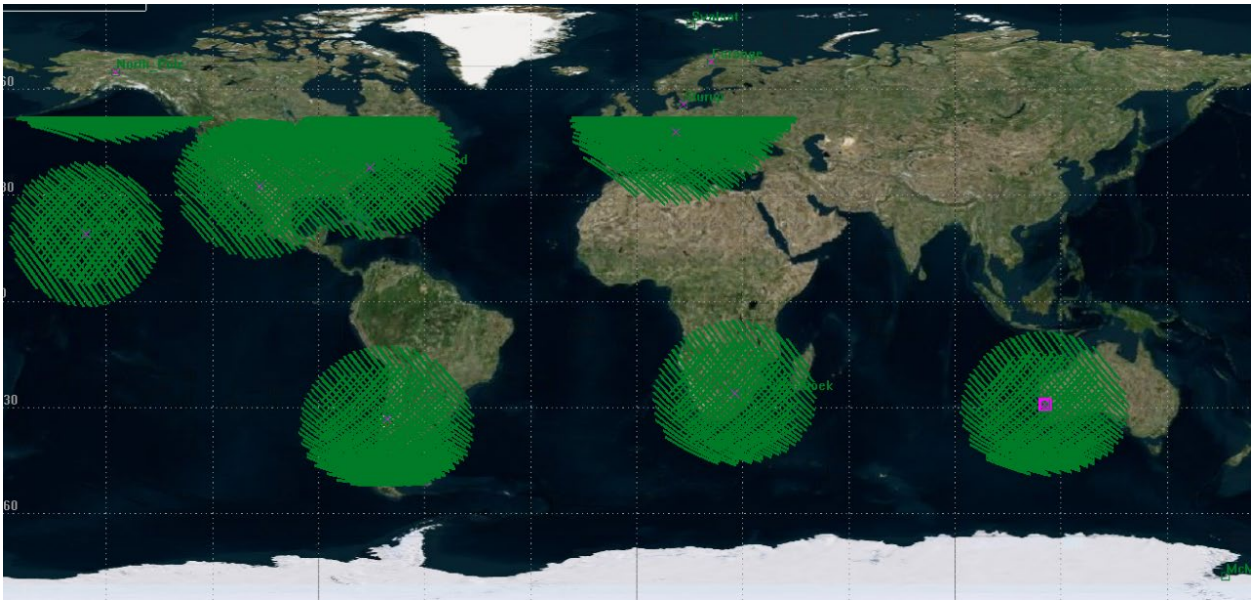

Figure 29 - NASA NEN stations with coverage zones (NASA, STK)

In addition to being comprised of all professional or commercial stations, many of them are located in places with direct sightlines to communicate with the ISS, and have wide fields of view. Even for heliosynchronous or polar orbits, the network contains multiple stations near the poles. The network may be well suited to more nominal orbits, but still has enough ground stations to

facilitate alternative mission options, with stations that provide better coverage in polar orbits or other high-inclination orbits (Thoman, Carter, 2016).

5.1.2 Transceiver

The transceiver interfaces with the payload instrument and onboard computer (OBC). It converts numerical data into signals and relays them to accessible ground stations. These ground stations in turn send commands to the OBC, which directs the NeAtO and its components. The strength of the transceiver determines the uplink and downlink capacities, which are the speeds at which data can be relayed to and received from the satellite by the coverage network. As a transceiver combines the functions of a radio receiver and a transmitter into one component, it is not obstructively large. This dual-function component, however, requires more power to run at maximum data rates, around 20V instead of 10V (IQ-Spacecom). The eLEO CubeSat project (JB-1801, 2018) utilized the ISIS VHF/UHF Full Duplex Transceiver shown in Figure 30.

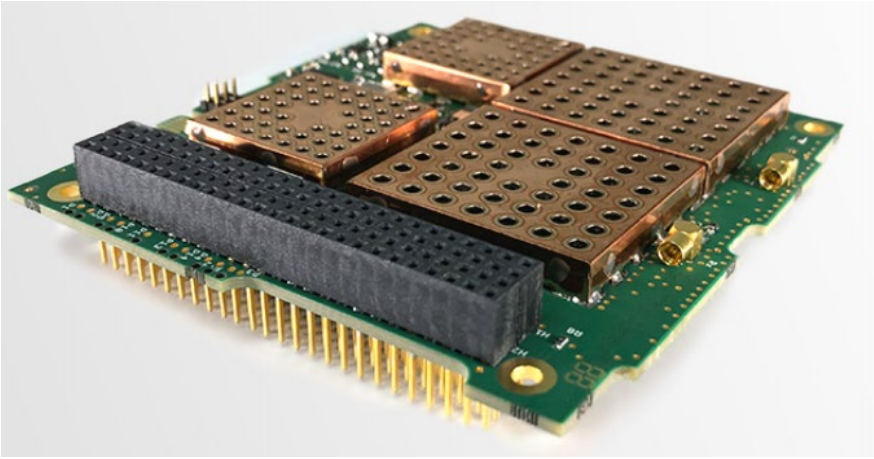

Figure 30 - VHF/UHF Duplex Transceiver (ISISpace)

At 0.0096 Mbps and 4W maximum operating conditions, this component is a good candidate for a CubeSat. It fits easily into an instrument cart, at 90mm x 96mm x 15mm, and with a defined downlink/uplink schedule, it provides a moderate data rate for a medium power draw.

Additionally, it can run only in receiving mode or at low power, down to 0.48W (ISISpace). This provides the baseline of the NeAtO project.

5.1.3 Antenna

The antenna allows transmission and reception of the physical signals for the CubeSat. There are a variety of antenna styles, falling into deployable or non-deploying components. Deployable antennas are lighter and require less power, at the expense of needing extra space to deploy their fixtures. Non-deployable antennas, also called patch antennas, take up less space and can thus be mounted in a variety of places. While they do not need to deploy long fixtures, patch antennas require more power and are heavier. As there is mounting space for deployable antennas in this project's CubeSat, the decreased power usage and mass is an attractive feature. Additionally, deployable antennas for CubeSat missions are readily available and come in various configurations for different applications, such as monopole for greater signal range and gain, or dipole or turnstile for greater coverage. The previous projects selected antennas for a balance between antenna gain and coverage (JB-1801, JB-1701). Such hybrid antennas mitigate the need to point the antenna in a specific direction. For any antenna type, but especially non-deployable, the placement is very important, as it will take up space that could otherwise be occupied by solar panels or sensors.

5.2 Hardware Selection

As the goal of the telecommunication subsystem is to provide the fastest possible data transfer for the CubeSat's mission, the primary figures of merit are size, speed, and power of the system. While a fast transfer rate is desired, the system's efficiency is limited by electric power available to the spacecraft. Hardware options were compiled from various suppliers, including Clyde Space, ISIS, Syrlinks, IQ Wireless, and EnduroSat.

5.2.1 Transceiver

Transceivers were compared first. Using a combination of separate transmitter and receiver was immediately disregarded, as having both components would practically double the capacity the subsystem occupies on an already small spacecraft. Between different transceivers, the comparison comes down to data speeds and mass. To get the most out of a given coverage pattern, the data speed should be maximized. The operational frequency capabilities were also compared consisting of common S-Band equipment which uses 2-4GHz, and newly developed X-Band equipment of 8-12GHz. X-Band communications operate at the higher frequency and offer much faster rates. The drawbacks of this equipment are increased mass and power requirements, over S-Band equipment (Beasly, 2014). Another consideration is Technology Readiness Level (TRL). While S-Band benefits from being a mature and fully realized technology, X-Band does not. In comparing equipment in both frequency ranges, there was notably less readily available information on the X-Band components. Table 6 shows a comparison between both transmitters and transceivers in S and X band. The bolded columns in both Table 6 and Table 7 indicate that these were the conditions selected for the mission. Of note are the power requirements and data rates. While the X-Band equipment looks very promising, most of those components lack detailed specification sheets, and have not flown on space missions.

Table 6 - Transceiver and Transmitter Comparison

	Pulsar STX	Pulsar XTX	ISIS High Data-rate S-band	**ISIS VHF uplink/UHF downlink Full Duplex Transceiver**	HISPICO	X-Band	XLink
Company	Clyde Space	Clyde Space	ISIS	**ISIS**	IQ Wireless	EnduroSat	IQ Spacecom
	Transmitter	Transmitter	Transmitter	**Transceiver**	Transmitter	Transmitter	Transceiver
Power	<5W	<15W	13W	**.48-4W**	4.5-15W	12W	15W
	6-12 V	6.2-17V	7-20 V	**6.5-20V**	3-5V	10-24.5V	7-18V
Mass	100g	130g	120g	**75g**	75g	270g	200g
Size (mm)	96x90x17.4	96x90x11.7	98.8x93.3x14.5	**90x96x15**	95x46x15	95.9x90.2x23.6	90x65x28
Temp (°C)	-25, +60	-25, +60	-40, +70	**-20, +60**	-40, +65		-20, +50
Max Rate Down	7.5 Mbps	50 Mbps	4.3 Mbps	**0.0096 Mbps**	1.06 Mbps	50 Mbps	25 Mbps
Max Rate Up				**0.0096 Mbps**			.064 Mbps
Band	S	X	S	**S**	S	X	X

The ISIS Full Duplex Transceiver was chosen for coverage estimates due to the abundance of relevant information on it, and that it has been the best choice in previous missions very similar to this.

5.2.3 Antenna

The selected antenna has to match the transceiver frequency range and not create any impingement with other components. The impingement concern is particularly important relative to the solar array, as that affects power generation if the antennas block sunlight from the panels. As the bus design of NeAtO is subject to change, the manner in which an antenna deploys, and *if*

it deploys, determines if the antenna is compatible. Patch style antennas have to be mounted externally. This conflicts with the power subsystem, as the external faces of NeAtO are needed for solar panel mounting. Considering those constraints, the mass and antenna range are the remaining concerns. Table 7 compares antenna options, both S and X-band.

Table 7 - Transceiver and Transmitter Comparison

	ISIS hybrid	X-BAND PATCH ANTENNA	SPAN-X-T2	Pulsar SANT
Company	**ISIS**	EnduroSat	Syrlinks	Clyde Space
Power	**3.3-5V**			
(Deploy Power)	**2W**			
Size (mm)	**98x98x7**	24x24x6.4		81.5x89x4.1
Mass	**100g**			50g
Temp (ºC)	**-20, +60**			
Notes	**Deployable**	Patch	Patch	Patch
Band	**S**	X	X	S
Range (km)	**3000**			

As the antenna must match the frequency range of the transceiver, an S-Band antenna must be selected. Regardless, the minimal number of flight-ready X-Band instruments and lack of technical information on them makes S-Band the frequency of choice. For NeAtO, the antenna is mounted externally, on the ram-facing (front) side. While the patch antenna is smaller and lighter, the ISIS Hybrid deploying style was selected. The Pulsar SANT lacked power requirements and antenna range, which are critical to the estimates conducted to acquire a data budget.

5.3 Coverage Estimates

The coverage estimates are central to finding the data budget of the mission. After data rate, the amount of data that can be sent and received depends on when and for how long access to the ground stations lasts. Systems ToolKit allows orbits and telecommunications access to be compared, the Astrogator and telecommunications access features being utilized to create estimates and detailed schedules of access points. This is significant to the telecom system, as the position of the CubeSat in coverage regions dictates if uplink/downlink is possible, and the duration of those accesses dictates the amount of data that can be transferred.

The STK scenario started on a mission start date of May 15th, 2020, at 17:00, with the satellite orbit being propagated from the parameters in Table 8. A transceiver and antenna were added to the satellite based on the data from the selected components. The NASA NEN ground stations were added by latitude and longitude, taking the terrain into account when calculating the view into space of each site. The coordinates of these sites are listed in Table 9.

Table 8 - STK Scenario Orbit Parameters

Apogee Altitude	440km
Perigee Altitude	200km
Inclination	51.6^{o}

Table 9 - Ground Station Coordinates

Station Name	**Lat (degrees)**	**Long (degrees)**	**Altitude (km)**
AGU3	-33.151	-70.666	0.733301
Dongara	-29.046	115.349	0.25047
Esrange	67.884	21.061	0.4417
Hartebeesthoek	-25.887	27.707	1.568221
McMurdo	-77.839	166.667	0.153
North_Pole	64.804	-147.5	0.16058
South_Point	19.014	-155.663	0.367878
Sturup	55.541	13.349	0.1
Svalsat	78.23	15.408	0.501378
Wallops_Island	37.923	-75.477	-0.01064
Weilheim	47.88	11.085	0.663392
White_Sands	32.541	-106.612	1.456545

Figure 31 shows the access periods over 24 hours in the mission. To create estimates of the data budget, the access from the cube satellite to the ground network was calculated and averaged over a time period. The total time inside coverage was then multiplied by the transceiver data rate to give a maximum possible data budget for the period. Once an estimated data coverage per orbit was found, it could be compared to estimates calculated for different orbits. The access periods in Figure 31 are represented by a binary state, with high points being times when NeAtO has access to a ground station, and low points being when it is out of range of the ground stations.

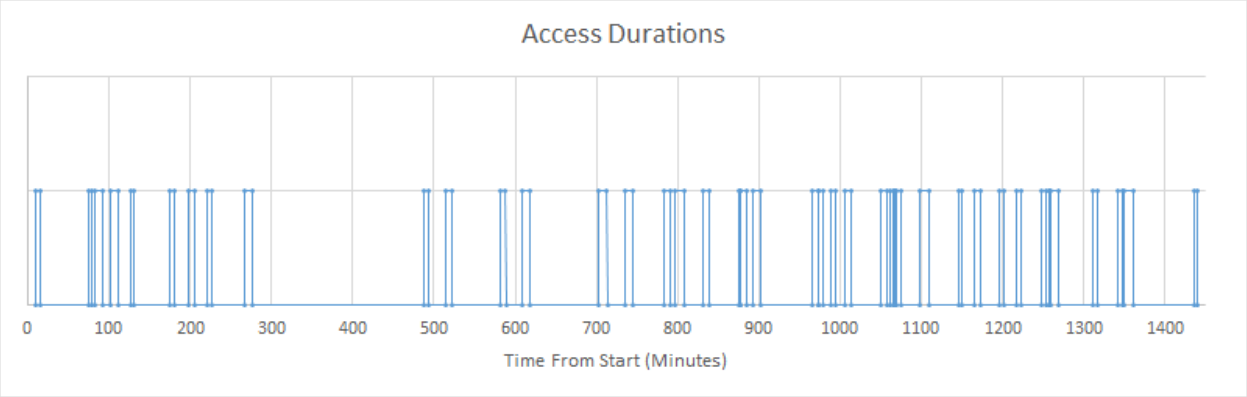

Figure 31 - Access periods to ground station network

5.4 Telecommunications Results

The average data budget for one orbit is approximately 11.52Mb, which makes the daily data budget just about 180Mb with max power. To consider the power constraint, the subsystem runs at ⅔ full capacity, which means that both power use and data rate will be reduced by a third. This works in conjunction with the payload on a data schedule so that all data that is generated can be downlinked in the same orbit period. This meets the subsystem requirements of downklinking as much data as possible, as fast as possible, without imposing a strain on the power subsystem that would drastically shorten the mission lifespan.

6. Environmental Effects Analysis

Heat physically limits the CubeSat and what it can accomplish in terms of mission longevity and orbital parameters. If the sun exposure is too much, or the drag induces too much heat, the CubeSat's physical structure and individual parts within the test bed are at risk of failure. Solar radiation pressure and ionized oxygen in the plasma environment demand that the CubeSat be specially coated for protection. This chapter aims to identify the environmental dangers of spaceflight and to provide explanations on how to protect the satellite during its mission.

6.1 Environmental Effects Overview

Extreme Low Earth Orbits (eLEOs) add more challenges for CubeSats which usually orbit much higher. Atmospheric winds and drag are present at such low altitudes. If the CubeSat deviates from its precise course, the mission could fail, as the CubeSat would burn up in the atmosphere.

The previous MQP “Design of CubeSats for Formation Flying & for Extreme Low Earth Orbit” (NAG-1801, MAD-1801, and JB-1801, 2018) used a number of techniques to prevent mission failure due to atmospheric interference. With an increased drag force, the MQP team found that a 4U CubeSat was required over the originally planned 3U design. This was because the velocity change at the desired altitude of 210km required more fuel for the thrusters. Using an array of micro pulsed plasma thrusters (μPPTs), the CubeSat could reorient itself at any time to ensure stability and control during atmospheric interference.

Systems ToolKit (STK) is used to recreate and simulate the environment of the CubeSat’s orbit. Systems Tool Kit contains many different density models for the atmosphere for any given orbit. With this simulation, the team can accurately model and graph the atmospheric drag, satellite temperature, magnetic flux, and power generation from the solar panels throughout each orbit.

Previously, MQPs in the past have suggested that atmospheric drag exists and solar winds can add a level of complexity for each orbit. Using MATLAB, the previous MQPs have calculated atmospheric drag and fuel consumption for each orbit, but they did not do a full analysis of each layer of the ionosphere and thermosphere.

6.2 Environmental Effects Research

This team's mission is to conduct research in the ionosphere with the miniaturized NIMS payload. The ionosphere ranges from about 50km to almost 1,000km during the most active hours in the day. The ionosphere gets its name from the fact that UV radiation from the sun activates, or ionizes, molecular oxygen (O) and nitric oxide (NO). This ionization process requires a lot of energy and superheats the particles up to 1000K, creating a plasma environment. The spacecraft will be operating in the F-region of the ionosphere to determine the relationship between the composition of the ionosphere and weather patterns in this region in order to predict geomagnetic storms and the impacts thereof upon global communications. The F-region consists of two sub-regions. The F1 layer is only present during daylight, existing at approximately 150-220km. Composed of a mixture of $O2^{+}$, NO^{+}, and atomic O^{+} ions and with an electron density of $5 \cdot 10^{5}$ free electrons/cm^{3}, it merges into the F2 layer at night and drops to roughly $1 \cdot 10^{4}$ free electrons/cm^{3}. The F2 layer is always present at 220-800km during the daytime, composed of mostly atomic oxygen ions, and will be where this spacecraft spends the majority of its mission. The nominal electron density is $2 \cdot 10^{6}$ free electrons/cm^{3}, but this region is unstable and variations often occur, especially during magnetic storms.

NeAtO's structural frame harbors all the delicate components that are necessary for the mission. Chromatic Conversion Coating (CCC) is a chemical process that can help with thermal properties, electrical contact resistance and corrosion performance. It has been found that using

CCCs that have a chromatic solution very close to the very near to the commercial chromating solution of Alodine 1200S, both the absorptivity and emissivity of the aluminum 7075-T6 can increase. Allowing for more efficient thermal loading and overall less heat in the structure.

6.3 Modeling Atmospheric Effects

The thermal model for the environmental analysis will be calculated using STK. Required input parameters include the desired orbit, Earth's albedo, the material's absorptivity and emissivity, dissipated heat from the internal components and spacecraft orientation. The thermal modeling from STK will provide an estimate of the temperature fluctuations experienced by the spacecraft throughout a given orbit. Accurate material properties are critical to the accuracy of the STK thermal model.

STK will also be used to analyze the magnetic flux per orbit in tandem with COMSOL Multiphysics. STK's Space Environments and Effects Tool (SEET) package contains a Geomagnetic Field tool for modeling Earth's magnetic field. It can provide a visual representation of magnetic field lines up to 120,000km above Earth, which provides more than enough coverage for this model. This Geomagnetic Field tool will produce a vector profile of the magnetic flux through the spacecraft during an orbit, which can then be entered as an input to COMSOL Multiphysics to analyze the effects of the Earth's magnetic field as well as any interference due to the magnetorquers on the spacecraft.

The structures team (NK-2001) selected Aluminium 7075-T6 for the custom 6U CubeSat frame and provided sources regarding the material properties. Using an Earth albedo of 0.34, a material absorptivity of 0.9, emissivity of 0.22 and dissipation of 14 watts, this team modeled the temperature. Figure 32 shows a maximum temperature of 314°C and a minimum of 96°C. This is

important because all internal components must function at these temperatures or insulation is needed to ensure proper function.

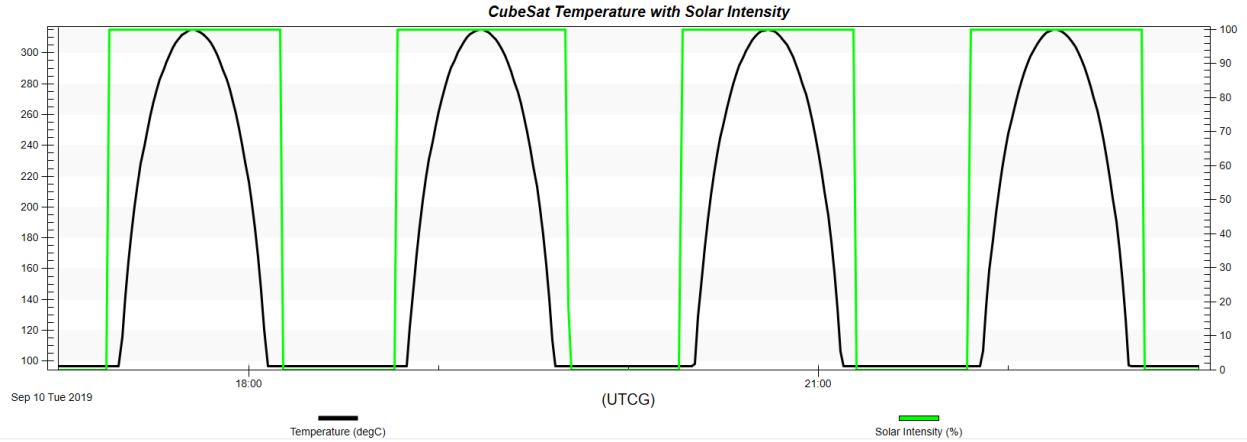

Figure 32 - NeAtO External Temperature Versus Solar Intensity

Most of the surface that will be exposed to solar radiation will be solar panels, thus having a slightly different temperature reading. The solar panels have a high absorptivity of 0.91, but have a ranging emissivity at each wavelength. While most of the radiation from the sun is in the visible spectrum, solar panels only emit frequencies in microwaves. This causes high levels of heat to build up on the surface of the solar panel. Proper ventilation and cooling must be present to ensure the panels do not overheat.

This team created a simulation for the CubeSat in COMSOL Multiphysics using the same parameters from STK (see Figure 33). The results showed a maximum temperature of 536K (263°C) on the ram-facing side. This maximum coincides nicely with the STK average satellite temperature reading since it falls below that range.

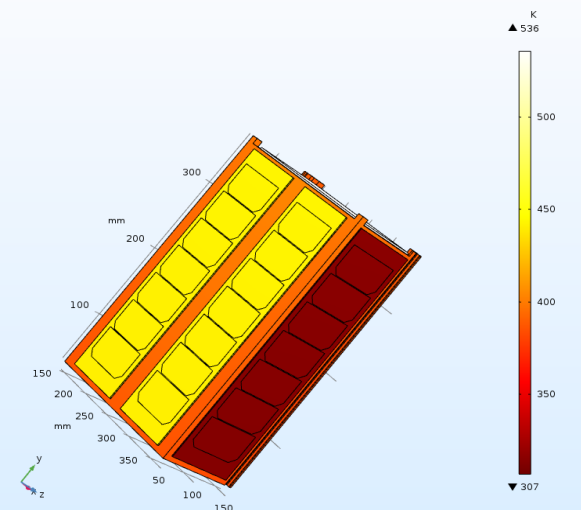

Figure 33 - NeAtO's Thermal Profile from COMSOL

While the COMSOL model matches the STK analysis, the results are misleading. The temperature range is high due to an error in modeling NeAtO. There was a plate added to the RAM facing side which creates much more drag, absorbs more heat and treats the vehicle as a closed box with no thermal venting. NeAtO's final design will have the payload replace the plate and two “holes” that will facilitate ventilation. This is crucial to sustaining a long-term mission and ensuring thermal stability throughout the internal components.

6.4 Magnetic Interference Modeling

The ADCS team (MAD-2001) chose to use magnetorquers to maintain attitude throughout the mission. These magnetorquers are functionally solenoids, with a ferrite alloy core wrapped in thin copper wire. When turned on, these magnetorquers create a magnetic field which acts against the Earth’s magnetic field, creating a net torque and rotating the spacecraft. This magnetic field is generated inside the CubeSat, which can potentially cause interference with sensitive instruments and components of the satellite, such as the onboard computer, the payload, the thrusters, and the magnetometer, the last of which helps to determine the attitude of the spacecraft by measuring

Earth's magnetic field. This team simulated the magnetic flux throughout the spacecraft in COMSOL in order to determine if magnetic shielding was necessary.

6.4.1 Modeling a Single Magnetorquer

For a baseline calculation, this team created the model of a single magnetorquer in COMSOL to analyze its internal magnetic flux and field lines, to guarantee that the model was accurate. The specifications sheet provided for the magnetorquer provided the magnetic moment, μ, the radius of the magnetorquer, the power and voltage required to run the magnetorquer, and the length of the magnetorquer. The current through the coil, I, was calculated using:

$$I = \frac{P}{V} \tag{8}$$

where P is the power in Watts, and V is the voltage applied. The number of turns, n, is calculated from:

$$n = \frac{\mu}{IA} \tag{9}$$

where I is the current, in amps, and A is the cross-sectional area in square meters, which results in 63,662 turns in the coil on the magnetorquer. These values, and the constants from the specification sheet, are listed in Table 10.

Table 10 - Constants for determination of turns in magnetorquer coil

Parameter	Value
Magnetic moment	$0.2Am^2$
Power	200mW
Voltage	5V
Current	0.04A

Radius	0.005m
Cross-sectional area	$7.85 \cdot 10^{-5} m^2$
Length	0.07m
Number of turns in coil	63662

Starting with a single cylinder aligned with the z-axis surrounded by a sphere defined as an infinite element (i.e. as a vacuum), the Magnetic and Electric Fields (mef) physics engine was applied within COMSOL. A Coil boundary condition was used on the lateral face of the magnetorquer to simulate the copper wire, avoiding the need to create a physical model of a coil. A start condition was specified for the coil, and the COMSOL model produced the models for magnetic flux density and magnetic field lines as shown below in Figures 34 and 35, respectively.

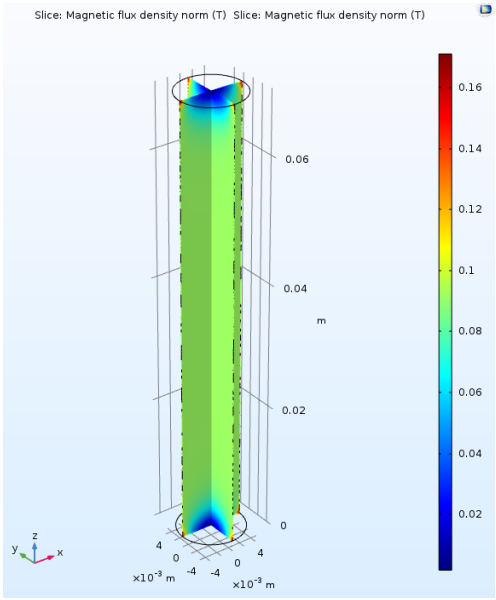

Figure 34 - Magnetic flux density in single magnetorquer

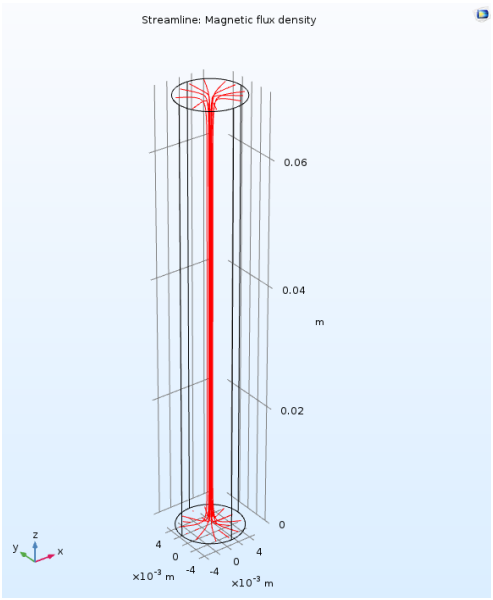

Figure 35 - Magnetic field lines inside single magnetorquer

The flux distribution internally, as shown in Figure 34, only decreases where the field lines diverge out of the ends of the magnetorquer due to end effects, remaining even throughout the rest

at a value of 0.092T. The field lines as shown in Figure 35 are consistent with expected results and would produce a magnetic field similar to a bar magnet.

Figure 36 shows the magnetic flux density inside the magnetorquer from its center (0 on the x-axis of the graph) to one end (0.035m on the x-axis of the graph). The internal magnetic flux density is constant through the magnetorquer up through 0.025m away from the center, at which point the end effects take over, which corresponds with the results of the prior two graphs.

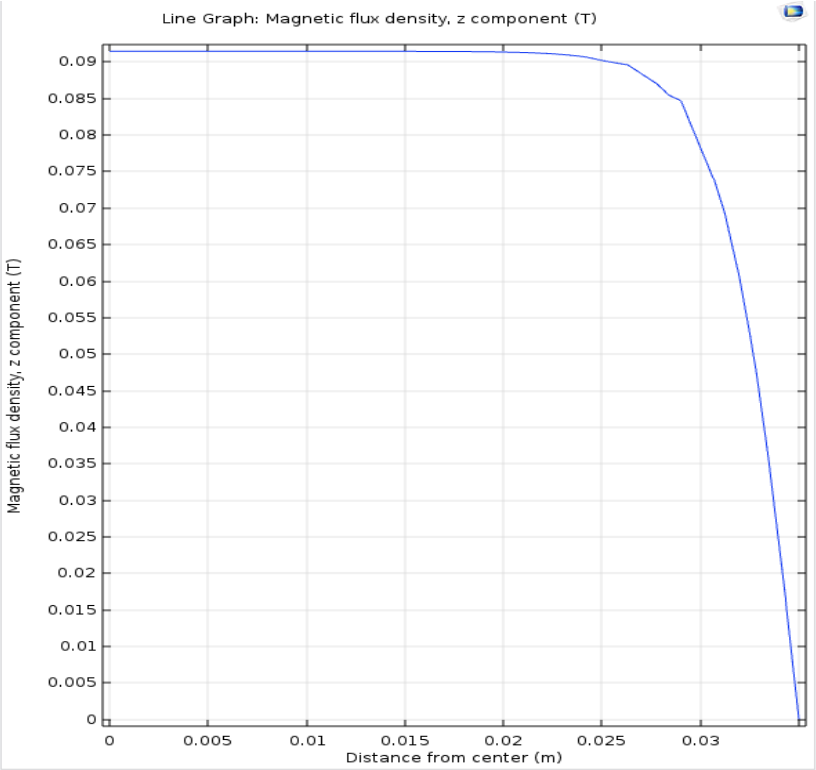

Figure 36 - Magnetic Flux Density vs. Distance Along the Z-Axis

6.4.2 Modeling the Earth's Background Magnetic Field

The next step was to place the defeatured frame of the CubeSat into COMSOL and simulate the effects of Earth's magnetic field to guarantee that the frame created negligible magnetic interference. The SolidWorks CAD file for the frame was exported as an .stp file and imported directly into COMSOL as its own object as shown in Figure 37. This object required an extremely

fine mesh as to account for the intricacies of the frame, which increased processing times for the physics engine. The CubeSat was placed in a sphere defined with vacuum conditions, and using the Magnetic Fields, No Currents (MFNC) COMSOL physics engine, a background magnetic field was defined at 0.04 T, to simulate Earth's magnetic field at this altitude. Although there is some interference due to the skeleton of the CubeSat, it amounts to only 0.02nT at most, which is well below any interference thresholds of the internal instruments, and only occurs localized to the frame itself.

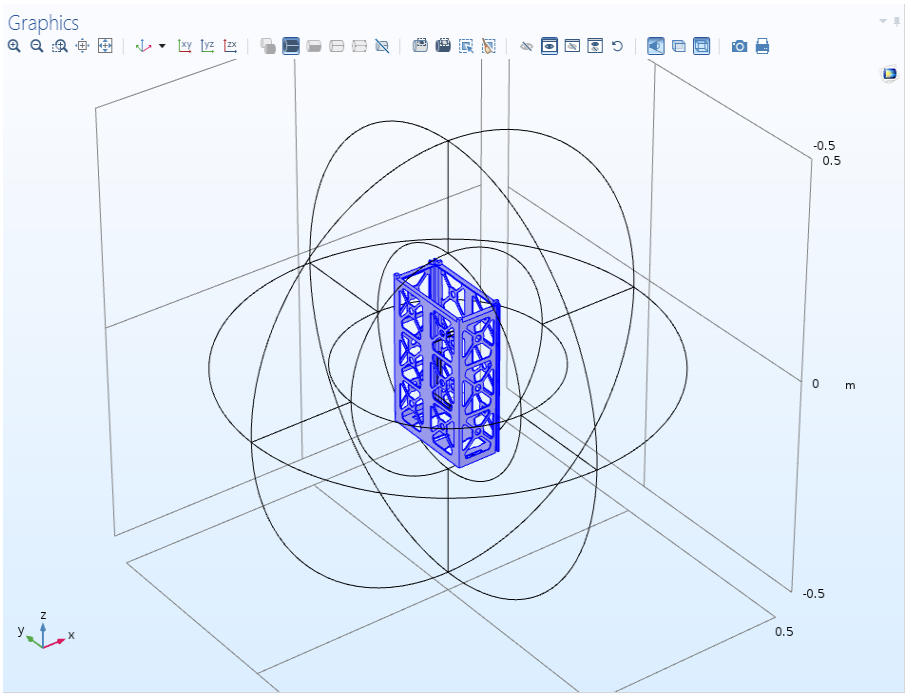

Figure 37 - Defeatured CubeSat skeleton in COMSOL

7. Thermal Vacuum Chamber Preliminary Research

This MQP is responsible for the preliminary design of a Thermal Vacuum Chamber (TVaC) with which to subject the structural and electrical of the spacecraft to thermal loading relevant to what it would experience during the mission profile. While the scope of this project is not to build and implement the TVC, the following section aims to lay the groundwork for future WPI CubeSat projects to use as reference in their own TVC design.

7.1 Testing Applications and Standards

Spacecraft experience extreme pressures and temperatures not found on Earth. Thermal Vacuum Chambers provide the means of testing the reliability and functionality of a spacecraft hardware under thermal cycling and low pressures. While similar analysis can be done in programs such as COMSOL and ANSYS, a TVC provides a means to physically demonstrate the environment and verify and validate simulations.

Tests are often done in compliance with standards established by the US Military. Relevant to this mission are the procedures defined in MIL-STD-202 and NASA-STD-7002b. The MIL-STD-202 describes methods with which to test the effects of isolated variables on electronic and electrical components while the NASA-STD-7002b describes methods to test the structural integrity of various materials within an accepted safety factor (NASA, 2018). The procedures presented in these documents are to be taken as guidelines; conducting the tests requires tailoring the methods as the situation requires.

With respect to MIL-STD-202, the vacuum chamber can comply with test methods 105C (Barometric Pressure) and 107G (Thermal Shock). 105G outlines the dangers high altitude flight can have on electric components. Low pressures may subject the components to dielectric-

withstanding-voltage failure, weaker electrical contacts, and high pressure differentials along seals. The air's increased thermal insulation mitigates heat transfer, thus internally generated heat will remain near its source. As a result of these effects, the dielectric constant (a measure electric insulation) of the component decreases (Department of Defense, 2002).

The Thermal Shock tests described in section 107G of the MIL-STD-202 can be used to explore the effects of extreme temperature cycling the CubeSat will undergo throughout its orbit. The application and distribution of heat on components over thermal cycles causes non-uniform deformation of various portions of the component. These deformations can lead to cracks, fillings leakage, weakened seals, and mechanical displacement of electrical materials (Department of Defense, 2002).

The NASA-STD-7002b document provides design and test requirements materials must adhere to in order to be flight-worthy, as decided by NASA administration. It specifies duration and safety factors for environmental testing, expected results from functional demonstrations, and margins of acceptable performance.

8. Conclusions, Recommendations, and Social Impacts

This chapter provides recommendations that will assist in future CubeSat projects and reveal effective solutions to the problems encountered in the design and analysis process by the various subsystems of NeATo. The chapter concludes with the educational impacts of the CubeSat technology.

8.1 Payload Summary

The INMS payload carried onboard the 6U NeATo maintained a duty cycle of 8.9% for the mission, turning on at 240 km altitude and off at 200 km altitude. This duty cycle produces 6.61 Mb of data per orbit, or 10.58 Mb data per day, which will be downloaded for analysis via the Ground Station Network. Collection profiles were planned for activation altitudes between perigee and 300 km. The 240-200 km duty cycle was selected in order to collect meaningful scientific data at the F1/F2 transition boundary in the ionosphere, while minimizing the power draw for various subsystems, ultimately achieving the design goal.

8.2 Propulsion and Orbital Analysis

Orbit analysis was performed using the STK software. The propulsion subsystem is based on the Busek BET-300P electrospray thruster. It is able perform an orbit transfer from the deployment from the ISS at an altitude of 400 km to an elliptical orbit with an apogee of 440 km and a perigee of 200 km. This orbit transfer requires approximately 35.2g of propellant. Once NeATo reaches the desired orbit, the propulsion subsystem allows it to stay in orbit for 45 days, using the remaining 28g of propellant. For comparison without propulsion our analysis shows that the NeATo would deorbit in 16 days.

8.3 Power Analysis

The power subsystem consists of Clyde Space's Photon-3U body mounted solar panels, Starbuck Nano-Plus EPS board, and Optimus-40 40Whr battery. The subsystem is capable of providing a consistent 17.5W for approximately 80 days from the beginning of the mission. This power is adequate to operate the rest of the subsystems at a reduced power. After 80 days, the battery is expected to completely drain and become unable to recover. The power subsystem can remain operational for twice as long the propulsion subsystem can, this does not mean the power budget for those first 45 day would change. As the telecommunications operation was deemed to have less of an effect on the success of the scientific mission than the ADCS and payload operation, it was the first subsystem to have its power budget reduced for the sake of prolonging the mission time.

8.4 Telecommunications Analysis

The telecommunication subsystem has an 180 Mb of daily downlink and uplink capacity. The subsystem can sustain this daily data rate for the entire mission on reduced power, for as long as the orbit and power level can be sustained. The reduced data option of the payload, and reduced power level of the telecom instruments do limit the mission productivity, but allow for a much longer lifespan than would be possible otherwise. This allows more data to be taken for a long period of time, which may produce more useful results.

8.5 Environmental Effects Analysis

Given the maximum temperature in sunlight, the metal frame of NeAtO will survive, but the solar panels could be at risk due to high absorptivity and high drag. Thermal shock also adds a level of complexity as the internal stress on each component and soldered wire can lead to

electronic failure. In order to fully understand the impact of thermal shock on NeAto, an experiment should be conducted in a thermal vacuum chamber. The environment produced can simulate the space environment and can show whether or not thermal shock will cause component failure. Meanwhile, the magnetorquers produce a magnetic flux density of 0.092 T, four orders of magnitude higher than Earth's background magnetic field. As a result, if the magnetic flux at a single component exceeds the component's own shielding, future projects will need to consider external shielding for mission survival.

8.6 Recommendations

The following section provides recommendations to be considered for future iterations on the NeATo CubeSat. They reflect the shortcomings of each subsystems' analysis and offer ideas for what will improve the process and results of those future missions.

1. General Project Management

- Define and share a master simulation file for all subsystem teams to utilize and modify as needed. This will keep teams from wasting time recreating simulations that have already been used elsewhere.

2. Payload

- Consider an inactive "survival period" where no data is collected for a number of orbits to allow for the battery to recharge in order to extend mission lifespan.

3. Propulsion

- Consider the use of propellant tanks to increase the amount of propellant available for the thruster. This will help increase the mission lifespan.

4. Power

- Take orbital decay into consideration. As the orbit decays, components which activate at lower altitudes draw power for larger portions of the orbit. A profile that addresses this issue will be more accurate.
- Select solar panels that cover the maximum surface area.
- Use the equation for solar panels' power generation to optimize the angle of incidence throughout the mission.

5. Telecommunications

- Be persistent and obtain full component specifications from suppliers.
- Make use of available X-Band equipment.
- Take orbital decay into consideration and address how it affects coverage windows.
- Look into the possibility of using multiple antenna and transceiver pairings to increase data rate.

6. Environmental Effects

- Perform a full 3-D COMSOL simulation of the CubeSat, with all three magnetorquers active, in order to determine magnetic flux upon each sensitive component.
- Perform magnetic impact analysis for various orbits considering variations in the Earth’s magnetic field.
- Consider the impacts of radioactive environments on the CubeSat, and guarantee essential components are radiation hardened if this is deemed an issue.

8.7 Social Impacts of CubeSats

CubeSats provide unique opportunities for students to gain hands-on experience through which they can exercise the skills and knowledge they have gained in a traditional lecture setting. More and more higher education STEM institutions are turning to project-based learning (PBL) to give their students a real-world understanding of the material. Studies have shown that PBL can lead to higher average examination scores; Freeman et al. (2015) claim that exam scores were increased by 6% in classes with active learning projects and that students in courses with solely traditional lecturing are 1.5 times more likely to fail out of that class (S. Freeman, S.L. Eddy, M. McDonough, M.K. Smith, N. Okoroafor, H. Jordt, and M.P. Wenderoth, 2014).

Not only is PBL a more effective method of teaching difficult material, it also places the students in a position they may never have been in before. CubeSats are specifically effective at exposing students to the complicated process of designing a multi-subsystem project. The design and functionality of any one subsystem is strongly linked to the design and function of the others. Creating a functioning CubeSat requires effective communication between project members and that each member has an understanding of the system as a whole. Compared to scientific missions that require large, complex spacecraft, CubeSat projects offer more leeway for success in several aspects of design that lends itself directly to an effective educational experience: missions often consist of simple orbital maneuvers and passive data collection; the satellite consists of few subsystems, all dedicated to completing the primary mission; the small frame and standardized sizing invoke a short construction timeline; and ambiguous or loosely defined mission characteristics encourage creative thinking (National Academies of Sciences, Engineering, and Medicine, 2016).

The educational benefits of a large CubeSat program can be seen on the campus of the University of North Dakota, where the OpenOrbiter Small Spacecraft Development Initiative (OOSSDI) launched in 2012. The program aims to demonstrate the opportunities in 1U NanoSatellites, which can be designed and constructed from off-the-shelf hardware for under $5,000. While it is easy to say that project-based programs like this help to give the students real-world experience, it is difficult to quantify just how much it actually affects the students' academic capabilities. According to Straub et al. (2013), there is a correlation between duration of participation in the program and various indicators of academic ability. The study surveyed students associated with OOSSDI and compared their self-reported improvement (not overall competency) in areas such as Technical Skill, Spacecraft Design, and Space Excitement with variables including years in the program, hours spent per week on the project, overall GPA, undergraduate/graduate status, and more (Straub & Whalen, 2014).

The main conclusions were that hours spent per week on OOSSDI, years participating in the program, and having the role as team lead all had a strong correlation with overall academic improvement. There was no significant correlation between GPA, undergraduate versus graduate students, and class level with aggregate growth. The variables which related to the students to their role and responsibility within OOSSDI all correlated with improvement while the variables defined independently of the students' connection to OOSSDI showed no correlation with improvement. Given these results, the study concluded that the NanoSat program had a positive influence on its students (Straub & Whalen, 2014).

At WPI over the past five years, three MQPs have been conducted on various Cubesat missions. Unlike large spacecraft, the availability of COTS components for Cubesats allowed the

students of these projects to proceed with a complete spacecraft design. The MQPs provided a realistic and unique exercise in spacecraft and mission design.

Works Cited

AAC Clyde Space. *Solar Panels - Photon* (2019, August 1). PDF. Retrieved from https://www.aac-clyde.space/assets/000/000/078/PHOTON_original.pdf?1564954830

AAC Clyde Space. *Battery - Optimus* (2019, August 1). PDF. Retrieved from https://www.aac-clyde.space/assets/000/000/079/OPTIMUS_original.pdf?1564954960

AAC Clyde Space. *Power Distribution and Conditioning Units - Starbuck-Nano* (2019, August 1). PDF. Retrieved from https://www.aac-clyde.space/assets/000/000/103/STARBUCK-NANO_original.pdf?1565681302

Agasid, E., Burton, R., Carlion, R., Defouw, G., Perez, A. D., Karacalioglu, A. G., … Weston, S. (2018, December). PDF. Moffett Field.

AGI . (2019, December). COLLADA Models. Retrieved from http://help.agi.com/stk/index.htm#vo/modelImport.htm.

AGI. Blender Modelling and Articulations for STK Users. (n.d). PDF.

Beasley, J., & Miller, G. M. (2014). *Modern electronic communication*. Harlow: Pearson.

Blandino, J.J., Martinez, N., Demetriou, M. A., Gatsonis, N. A., Paschalidis, N., "Feasibility for Orbital Life Extension of a CubeSat Flying in the Lower Thermosphere", *Journal of Spacecraft and Rockets*, Vol. 53, No. 5, pp. 864-875, 2016. DOI:10.2514/1.A33462

Clark, C., & Simon, E. (2007). Evaluation of Lithium Polymer Technology for Small Satellite Applications. Retrieved December 17, 2019, from https://digitalcommons.usu.edu/smallsat/2007/all2007/66/

Courtney, Daniel G., et al. "Electrospray Thrusters for Small Spacecraft Control: Pulsed and Steady State Operation." *2018 Joint Propulsion Conference*, 2018, doi:10.2514/6.2018-4654.

Curci, E. A., Jacobson, J. B., Slabinski, K. M., & Schlack, W. T. (2017). Design and Analysis for the Sphinx-NG CubeSat. Retrieved from https://digitalcommons.wpi.edu/mqp-all/3638

Department of Defense. Test Method Standard: Electric and Electronic Component Parts (2002). Columbus, OH.

Dunbar, Brian. "Ion Propulsion." *NASA*, NASA, 18 Aug. 2015, Retrieved from www.nasa.gov/centers/glenn/about/fs21grc.html.

Electrospray Thrusters Boost Efficiency, Precision. *NASA*, NASA, Retrieved from spinoff.nasa.gov/Spinoff2016/ip_9.html.

Freeman, S., Eddy, S.L., McDonough, M., Smith, M.K., Okoroafor, N., Jordt, H., and Wenderoth, M.P. (2014). Active learning increases student performance in science, engineering, and mathematics, Proceedings of the National Academy of Sciences 111(23):8410-8415.

Garner, R. (2018, October 22). Dellingr: The Little CubeSat That Could. Retrieved from https://www.nasa.gov/feature/goddard/2018/dellingr-the-little-cubesat-that-could

Gatsonis, N.A., Ye, L., Blandino, J.J., Demetriou, M., Paschalidis, N., "Micro Pulsed Plasma Thrusters for Attitude Control of a Low Earth Orbiting CubeSat," *Journal of Spacecraft and Rockets*, Vol. 53, No. 1, pp. 57-73, 2016. DOI: 10.2514/1.A33345.

Hall, Nancy. "Solid Rocket Engine." *NASA*, NASA, Retrieved from www.grc.nasa.gov/WWW/K-12/airplane/srockth.html.

Henry, C. (2019, September 7). SpaceX says more Starlink orbits will speed service, reduce launch needs. Retrieved from https://spacenews.com/spacex-says-more-starlink-orbits-will-speed-service-reduce-launch-needs/

Horvath, G., Marosy, G., Glisics, S., & Czifra, D. (2012). Battery characterization for CubeSat missions with battery tester application. *2012 13th Biennial Baltic Electronics Conference*. doi: 10.1109/bec.2012.6376824

Jeffrey, Davidson, Ryan, Earle, Greg, Halford, … Rob. (2018, July). PetitSat - a 6U CubeSat to examine the link between MSTIDs and ionospheric plasma density enhancements. Retrieved from https://ui.adsabs.harvard.edu/abs/2018cosp...42E1773K/abstract

Jenner, L. (2017, May 9). NASA Team Pursues Blobs and Bubbles with New PetitSat Mission. Retrieved from https://www.nasa.gov/feature/goddard/2017/nasa-team-pursues-blobs-and-bubbles-with-new-petitsat-mission

Jenner, L. (2017, August 2). NASA Set to Launch Dellingr. Retrieved from https://www.nasa.gov/feature/goddard/2017/nasa-set-to-launch-dellingr-cubesat-purposely-designed-to-improve-reliability-of-small-0

JPL: NASA. (n.d.). Missions. Retrieved from https://www.jpl.nasa.gov/cubesat/missions/

K., S. (2009, January 1). THERMOPHYSICAL AND ELECTRICAL PROPERTIES OF CHROMATE CONVERSION COATINGS ON ALCLAD AA7075-T6 ALUMINUM ALLOY. Retrieved from https://www.sid.ir/en/Journal/ViewPaper.aspx?ID=175658

Kalde, J. (2012, July). *System architecture of the ESTCube-1 satellite power system*. Retrieved from http://jaanus.tech-thing.org/space/more-details-electrical-power-system/

Kant, A. B., Nichols, J. J., Mancinelli, L. J., Knodler, M. J., Abad, M. F., Escalante-Hurtado, M., & Crockett, R. C. (2018). Design and Analysis of CubeSats in Low Earth Orbit. Retrieved from https://digitalcommons.wpi.edu/mqp-all/3885

Kewen Z., Gatsonis, N.A., Blandino, J. J., Demetriou, M. A., "Nanosat Orbit Raising and Rendezvous Using a Continuous-Thrust Controller," AIAA 2017-0163, 55th AIAA Aerospace Sciences Meeting, Grapevine TX, Jan. 9-13, 2017.

Loff, S. (2015, July 22). CubeSats Overview. Retrieved from https://www.nasa.gov/mission_pages/cubesats/overview.

Markets and Markets. (n.d.). CubeSat Market. Retrieved from https://www.marketsandmarkets.com/Market-Reports/cubesat-market-58068326.html?gclid=Cjw

Missions Launched. Retrieved from http://www.polysat.org/launched

Monopropellant Rocket Engines. *Monopropellant Rocket Engines | Aerojet Rocketdyne*, www.rocket.com/space/space-power-propulsion/monopropellant-rocket-engines.

Moorthy, A.K., J. J. Blandino, M. A. Demetriou, N. A. Gatsonis, "Extended Orbital Flight of a CubeSat in the Lower Thermosphere with Active Attitude Control", AIAA 2019-1518, AIAA Scitech 2019 Forum, January 2019. DOI: 10.2514/6.2019-1518.

Moorthy, A.K., J. J. Blandino, M. A. Demetriou, N. A. Gatsonis, "Orbit Maintenance and Attitude Control for a CubeSat Flying in the Lower Thermosphere", AIAA 2018-5404, AIAA Space 2018, September, 2018. DOI: 10.2514/6.2018-5404.

NASA. *State of the Art Small Spacecraft Technology.* (2018, December). PDF. Retrieved from https://www.nasa.gov/sites/default/files/atoms/files/soa2018_final_doc.pdf

National Academies of Sciences, Engineering, and Medicine. 2016. Achieving Science with CubeSats: Thinking Inside the Box. Washington, DC: The National Academies Press. doi:10.17226/23503

Navarathinam, N., Lee, R., & Chesser, H. (2011). Characterization of Lithium-Polymer batteries for CubeSat applications. *Acta Astronautica*, 68(11-12), 1752–1760. doi: 10.1016/j.actaastro.2011.02.004

NSF. Award Search: Award#1719200 - Collaborative Research: RAPID: Exocube 2 - A Cubesat to Measure In-situ the Global Distribution of Light Species Densities in the Exosphere. Retrieved from https://www.nsf.gov/awardsearch/showAward?AWD_ID=1719200

NSF. *National Science Foundation Annual Report* (2013). PDF. Wallops Island. Retrieved from https://www.nsf.gov/geo/ags/uars/cubesat/nsf-nasa-annual-report-cubesat-2013.pdf

Pultarova, T. (2017, April 19). Could Cubesats Trigger a Space Junk Apocalypse? Retrieved from https://www.space.com/36506-cubesats-space-junk-apocalypse.html.

Rodriguez, M., Paschalidis, N., Jones, S., Sittler, E., Chornay, D., & Uribe, P. *Miniaturized Ion and Neutral Mass Spectrometer for CubeSat Atmospheric Measurements.* (2016, August 6). PDF. Retrieved from: https://ntrs.nasa.gov/archive/nasa/casi.ntrs.nasa.gov/20160010304.pdf

Spectrolab. (2018, July 16). PDF. Sylmar, California.

Straub, J., & Whalen, D. (2014). Evaluation of the Educational Impact of Participation Time in a Small Spacecraft Development Program. *Education Sciences*, *4*(1), 141–154. MDPI AG. Retrieved from http://dx.doi.org/10.3390/educsci4010141

Thoman, B. E., & Carter, D. L. (2016, February 24). Near Earth Network (NEN) Users' Guide. Retrieved from https://sbir.gsfc.nasa.gov/sites/default/files/453-NENUG R2.pdf

Wall, M. (2019, April 24). Meet OSCaR: Tiny Cubesat Would Clean Up Space Junk. Retrieved from https://www.space.com/space-junk-cleanup-cubesat-oscar.html.

Wertz, J. R., & Larson, W. J. (1999). *Space mission analysis and design* (3rd ed.). Torrance, CA: Microcosm.

Appendices

Appendix A: Battery Charge Code

2/22/20 1:50 PM C:\Users\Techstars\D...\MQP Power Script.m 1 of 5

```
clear all; clc;

T = readtable('C:\Users\Techstars\Documents\MQP Power to be Imported to MATLABv3.xlsx');
%Load Table

%% Create Basic Data

%Set up table data as matrices
Time = table2array(T(:,1));
Power_Gen = table2array(T(:,2));
Alt = table2array(T(:,3));

%Set up Power Draw
Power_Draw = ones(height(T),1)*5.575; %5.575 comes from always on components; can change
to 5.175 for only 1 magnetorquer

%The following loop handles payload on/off times (uses 1.8 watts)
for n = 1:length(Alt)
    if n == 1
        if Alt(n) <=240
            if Alt(n+1) < Alt(n)
            Power_Draw(n) = Power_Draw(n)+1.8;
            end
        end
    elseif Alt(n) <= 240
        if Alt(n-1) > Alt(n)
            Power_Draw(n) = Power_Draw(n)+1.8;
        end
    end
end

%The following loop handles the telecoms on/off times (peak power, 6W
%total, estimated based off of first 10 orbits)
loop = 0;
for n = 1:length(Alt)
    if n == 1
        Power_Draw(n) = Power_Draw(n);
    elseif datetime(2020,5,15,17,9,10,454)+minutes(902*loop)+seconds(13*loop)
+milliseconds(971*loop) <= Time(n) && Time(n) <= datetime(2020,5,15,17,16,16,989)+minutes
(902*loop)+seconds(13*loop)+milliseconds(971*loop)
        Power_Draw(n) = Power_Draw(n)+6;
    elseif datetime(2020,5,15,18,14,30,371)+minutes(902*loop)+seconds(13*loop)
+milliseconds(971*loop) <= Time(n) && Time(n) <= datetime(2020,5,15,18,18,50,212)+minutes
(902*loop)+seconds(13*loop)+milliseconds(971*loop)
        Power_Draw(n) = Power_Draw(n)+6;
    elseif datetime(2020,5,15,18,22,58,388)+minutes(902*loop)+seconds(13*loop)
+milliseconds(971*loop) <= Time(n) && Time(n) <= datetime(2020,5,15,18,31,31,795)+minutes
(902*loop)+seconds(13*loop)+milliseconds(971*loop)
        Power_Draw(n) = Power_Draw(n)+6;
    elseif datetime(2020,5,15,18,41,46,586)+minutes(902*loop)+seconds(13*loop)
+milliseconds(971*loop) <= Time(n) && Time(n) <= datetime(2020,5,15,18,51,54,540)+minutes
```

```
(902*loop)+seconds(13*loop)+milliseconds(971*loop)
        Power_Draw(n) = Power_Draw(n)+6;
    elseif datetime(2020,5,15,19,7,40,007)+minutes(902*loop)+seconds(13*loop)↙
+milliseconds(971*loop) <= Time(n) && Time(n) <= datetime(2020,5,15,19,10,17,920)+minutes↙
(902*loop)+seconds(13*loop)+milliseconds(971*loop)
        Power_Draw(n) = Power_Draw(n)+6;
    elseif datetime(2020,5,15,19,53,56,145)+minutes(902*loop)+seconds(13*loop)↙
+milliseconds(971*loop) <= Time(n) && Time(n) <= datetime(2020,5,15,20,1,20,508)+minutes↙
(902*loop)+seconds(13*loop)+milliseconds(971*loop)
        Power_Draw(n) = Power_Draw(n)+6;
    elseif datetime(2020,5,15,20,18,8,673)+minutes(902*loop)+seconds(13*loop)↙
+milliseconds(971*loop) <= Time(n) && Time(n) <= datetime(2020,5,15,20,25,35,525)+minutes↙
(902*loop)+seconds(13*loop)+milliseconds(971*loop)
        Power_Draw(n) = Power_Draw(n)+6;
    elseif datetime(2020,5,15,20,40,20,697)+minutes(902*loop)+seconds(13*loop)↙
+milliseconds(971*loop) <= Time(n) && Time(n) <= datetime(2020,5,15,20,47,5,824)+minutes↙
(902*loop)+seconds(13*loop)+milliseconds(971*loop)
        Power_Draw(n) = Power_Draw(n)+6;
    elseif datetime(2020,5,15,21,26,42,856)+minutes(902*loop)+seconds(13*loop)↙
+milliseconds(971*loop) <= Time(n) && Time(n) <= datetime(2020,5,15,21,37,13,865)+minutes↙
(902*loop)+seconds(13*loop)+milliseconds(971*loop)
        Power_Draw(n) = Power_Draw(n)+6;
    elseif datetime(2020,5,16,1,6,55,777)+minutes(902*loop)+seconds(13*loop)+milliseconds↙
(971*loop) <= Time(n) && Time(n) <= datetime(2020,5,16,1,12,52,388)+minutes(902*loop)↙
+seconds(13*loop)+milliseconds(971*loop)
        Power_Draw(n) = Power_Draw(n)+6;
    elseif datetime(2020,5,16,1,34,58,073)+minutes(902*loop)+seconds(13*loop)↙
+milliseconds(971*loop) <= Time(n) && Time(n) <= datetime(2020,5,16,1,42,32,658)+minutes↙
(902*loop)+seconds(13*loop)+milliseconds(971*loop)
        Power_Draw(n) = Power_Draw(n)+6;
    elseif datetime(2020,5,16,1,36,59,831)+minutes(902*loop)+seconds(13*loop)↙
+milliseconds(971*loop) <= Time(n) && Time(n) <= datetime(2020,5,16,1,42,46,411)+minutes↙
(902*loop)+seconds(13*loop)+milliseconds(971*loop)
        Power_Draw(n) = Power_Draw(n)+6;
    elseif datetime(2020,5,16,2,40,57,961)+minutes(902*loop)+seconds(13*loop)↙
+milliseconds(971*loop) <= Time(n) && Time(n) <= datetime(2020,5,16,2,48,19,736)+minutes↙
(902*loop)+seconds(13*loop)+milliseconds(971*loop)
        Power_Draw(n) = Power_Draw(n)+6;
    elseif datetime(2020,5,16,3,8,30,030)+minutes(902*loop)+seconds(13*loop)+milliseconds↙
(971*loop) <= Time(n) && Time(n) <= datetime(2020,5,16,3,17,29,636)+minutes(902*loop)↙
+seconds(13*loop)+milliseconds(971*loop)
        Power_Draw(n) = Power_Draw(n)+6;
    elseif datetime(2020,5,16,3,9,28,749)+minutes(902*loop)+seconds(13*loop)+milliseconds↙
(971*loop) <= Time(n) && Time(n) <= datetime(2020,5,16,3,18,0,216)+minutes(902*loop)↙
+seconds(13*loop)+milliseconds(971*loop)
        Power_Draw(n) = Power_Draw(n)+6;
    elseif datetime(2020,5,16,3,17,39,723)+minutes(902*loop)+seconds(13*loop)↙
+milliseconds(971*loop) <= Time(n) && Time(n) <= datetime(2020,5,16,3,18,19,733)+minutes↙
(902*loop)+seconds(13*loop)+milliseconds(971*loop)
        Power_Draw(n) = Power_Draw(n)+6;
    elseif datetime(2020,5,16,4,43,12,060)+minutes(902*loop)+seconds(13*loop)↙
```

```
+milliseconds(971*loop) <= Time(n) && Time(n) <= datetime(2020,5,16,4,52,36,294)+minutes↙
(902*loop)+seconds(13*loop)+milliseconds(971*loop)
        Power_Draw(n) = Power_Draw(n)+6;
    elseif datetime(2020,5,16,4,43,16,976)+minutes(902*loop)+seconds(13*loop)↙
+milliseconds(971*loop) <= Time(n) && Time(n) <= datetime(2020,5,16,4,52,44,034)+minutes↙
(902*loop)+seconds(13*loop)+milliseconds(971*loop)
        Power_Draw(n) = Power_Draw(n)+6;
    elseif datetime(2020,5,16,5,15,20,928)+minutes(902*loop)+seconds(13*loop)↙
+milliseconds(971*loop) <= Time(n) && Time(n) <= datetime(2020,5,16,5,25,2,136)+minutes↙
(902*loop)+seconds(13*loop)+milliseconds(971*loop)
        Power_Draw(n) = Power_Draw(n)+6;
    elseif datetime(2020,5,16,6,3,44,603)+minutes(902*loop)+seconds(13*loop)+milliseconds↙
(971*loop) <= Time(n) && Time(n) <= datetime(2020,5,16,6,10,11,974)+minutes(902*loop)↙
+seconds(13*loop)+milliseconds(971*loop)
        Power_Draw(n) = Power_Draw(n)+6;
    elseif datetime(2020,5,16,6,17,31,057)+minutes(902*loop)+seconds(13*loop)↙
+milliseconds(971*loop) <= Time(n) && Time(n) <= datetime(2020,5,16,6,27,16,685)+minutes↙
(902*loop)+seconds(13*loop)+milliseconds(971*loop)
        Power_Draw(n) = Power_Draw(n)+6;
    elseif datetime(2020,5,16,6,17,55,228)+minutes(902*loop)+seconds(13*loop)↙
+milliseconds(971*loop) <= Time(n) && Time(n) <= datetime(2020,5,16,6,27,53,556)+minutes↙
(902*loop)+seconds(13*loop)+milliseconds(971*loop)
        Power_Draw(n) = Power_Draw(n)+6;
    elseif datetime(2020,5,16,6,50,46,363)+minutes(902*loop)+seconds(13*loop)↙
+milliseconds(971*loop) <= Time(n) && Time(n) <= datetime(2020,5,16,6,59,13,284)+minutes↙
(902*loop)+seconds(13*loop)+milliseconds(971*loop)
        Power_Draw(n) = Power_Draw(n)+6;
    elseif datetime(2020,5,16,7,36,16,322)+minutes(902*loop)+seconds(13*loop)↙
+milliseconds(971*loop) <= Time(n) && Time(n) <= datetime(2020,5,16,7,36,53,321)+minutes↙
(902*loop)+seconds(13*loop)+milliseconds(971*loop)
        Power_Draw(n) = Power_Draw(n)+6;
    elseif datetime(2020,5,16,7,37,12,170)+minutes(902*loop)+seconds(13*loop)↙
+milliseconds(971*loop) <= Time(n) && Time(n) <= datetime(2020,5,16,7,45,27,597)+minutes↙
(902*loop)+seconds(13*loop)+milliseconds(971*loop)
        Power_Draw(n) = Power_Draw(n)+6;
    elseif datetime(2020,5,16,7,52,4,388)+minutes(902*loop)+seconds(13*loop)+milliseconds↙
(971*loop) <= Time(n) && Time(n) <= datetime(2020,5,16,8,0,39,633)+minutes(902*loop)↙
+seconds(13*loop)+milliseconds(971*loop)
        Power_Draw(n) = Power_Draw(n)+6;
    elseif datetime(2020,5,16,7,52,29,225)+minutes(902*loop)+seconds(13*loop)↙
+milliseconds(971*loop) <= Time(n) && Time(n) <= datetime(2020,5,16,8,2,13,971)+minutes↙
(902*loop)+seconds(13*loop)+milliseconds(971*loop)
        Power_Draw(n) = Power_Draw(n)+6;
    elseif datetime(2020,5,16,7,52,29,225)+minutes(902*loop)+seconds(13*loop)↙
+milliseconds(971*loop) <= Time(n-1) && Time(n-1) <= datetime(2020,5,16,8,2,13,971) ↙
+minutes(902*loop)+seconds(13*loop)+milliseconds(971*loop)
        loop = loop+1;
    end
end

%The following loop handles thruster on/off times for orbital maintenance
```

```
%(4 engines, .5W each)
for n = 1:length(Alt)
    if n == 1
        if Alt(n) <= 250
            if Alt(n+1) < Alt(n)
            Power_Draw(n) = Power_Draw(n)+2;
            end
        end
    elseif Alt(n) <= 250
        if Alt(n-1) > Alt(n)
            Power_Draw(n) = Power_Draw(n)+2;
        end
    end
end

Gain_Draw_Difference = Power_Gen-Power_Draw;

%Create Plot To Show Power Gen, Draw, and Altitude
figure
yyaxis left
plot(Time,Power_Gen,Time,Power_Draw)
title('Power Generation, Power Draw, & Altitude vs. Time')
xlabel('Time')
ylabel('Power (W)')
yyaxis right
plot(Time, Alt)
ylim([200 450])
ylabel('Altitude (km)')
legend('Power Generation', 'Power Draw', 'Altitude')

%Create Plot To Show Net Power Gain/Draw over Time
figure
plot(Time,Gain_Draw_Difference)
title('Net Power Gain/Draw vs. Time')
xlabel('Time')
ylabel('Power (W)')

%% Battery Charge

Gain_Draw_Difference = Gain_Draw_Difference*(1/60); %Convert Watts To Watt-Hours

Charge = zeros(length(Alt),1); %Establish charge matrix
Charge(1,1) = 80; %Establish initial full charge
Excess_Power = zeros(length(Alt),1); %Establish matrix to see if there'll be excess power↙
(in Whr), only purpose is for me to look at

%Apply power gain/draw to battery
for n = 1:length(Alt)
    if n == 1
        Charge(n) = Charge(n)+Gain_Draw_Difference(n);
    else
```

```
        Charge(n) = Charge(n-1)+Gain_Draw_Difference(n);
    end
    if Charge(n) >= 80
        Excess_Power(n) = Charge(n)-80;
        Charge(n) = 80;
    end
    if Charge(n) <= 0
        Charge(n) = 0;
    end
end

%Set up Battery Discharge Plot
figure
plot(Time,Charge)
title('Battery Charge vs. Time')
xlabel('Time')
ylabel('Power (Wh)')
```

Appendix B: Sample STK Data for Battery Charge

Time (UTCG)	Power (W)	Altitude (km)
5/15/2020 17:13	0	300.765076
5/15/2020 17:14	0	292.308806
5/15/2020 17:15	0	283.930238
5/15/2020 17:16	0	275.678954
5/15/2020 17:17	0	267.605695
5/15/2020 17:18	7.526	259.761928
5/15/2020 17:19	7.687	252.199365
5/15/2020 17:20	7.25	244.969447
5/15/2020 17:21	6.975	238.122792
5/15/2020 17:22	6.845	231.708628
5/15/2020 17:23	6.921	225.774203
5/15/2020 17:24	7.206	220.364205
5/15/2020 17:25	7.604	215.520179
5/15/2020 17:26	8.147	211.279974
5/15/2020 17:27	8.783	207.677224
5/15/2020 17:28	9.49	204.740865

5/15/2020 17:29	10.236	202.494725
5/15/2020 17:30	10.996	200.957168
5/15/2020 17:31	11.749	200.14082
5/15/2020 17:32	12.502	200.052385
5/15/2020 17:33	13.218	200.692536
5/15/2020 17:34	13.906	202.055912
5/15/2020 17:35	14.548	204.131195
5/15/2020 17:36	15.134	206.901286
5/15/2020 17:37	15.682	210.343561
5/15/2020 17:38	16.16	214.430204
5/15/2020 17:39	16.581	219.128615
5/15/2020 17:40	16.923	224.401872
5/15/2020 17:41	17.216	230.209246
5/15/2020 17:42	17.418	236.50675
5/15/2020 17:43	17.567	243.247711
5/15/2020 17:44	17.631	250.383358
5/15/2020 17:45	17.622	257.863404
5/15/2020 17:46	17.552	265.636623

5/15/2020 17:47	17.407	273.651403
5/15/2020 17:48	17.198	281.85627
5/15/2020 17:49	16.903	290.200375
5/15/2020 17:50	16.554	298.63394
5/15/2020 17:51	16.143	307.108653
5/15/2020 17:52	15.658	315.578016
5/15/2020 17:53	15.125	323.997636
5/15/2020 17:54	14.542	332.325472
5/15/2020 17:55	13.911	340.522015
5/15/2020 17:56	13.236	348.550432
5/15/2020 17:57	12.54	356.376653
5/15/2020 17:58	11.805	363.96941
5/15/2020 17:59	11.08	371.300239
5/15/2020 18:00	10.318	378.343443
5/15/2020 18:01	9.598	385.076016
5/15/2020 18:02	8.903	391.477543
5/15/2020 18:03	8.261	397.530069
5/15/2020 18:04	7.703	403.217956

5/15/2020 18:05	7.274	408.527713
5/15/2020 18:06	6.982	413.447822
5/15/2020 18:07	6.847	417.96856
5/15/2020 18:08	6.892	422.081808
5/15/2020 18:09	7.112	425.780869
5/15/2020 18:10	7.495	429.060294
5/15/2020 18:11	7.999	431.915706
5/15/2020 18:12	8.582	434.343644
5/15/2020 18:13	0.285	436.341425
5/15/2020 18:14	0	437.90701
5/15/2020 18:15	0	439.038906
5/15/2020 18:16	0	439.736076